(12)

AMMRC TR 78-14
BRITTLE MATERIALS DESIGN, HIGH TEMPERATURE GAS TURBINE

Volume 1 Ceramic Component Fabrication and Demonstration

Technical Report By:

Arthur F. McLean, Ford Motor Company, Dearborn, Michigan 48121
Robert R. Baker, Ford Motor Company, Dearborn, Michigan 48121

March, 1978

Interim Report Number 12, January 1, 1977 to September 30, 1977

Contract Number DAAG 46-71-C-0162

Sponsored by the Defense Advanced Research Projects Agency, Department of Defense, and the Division of Transportation Energy Conservation, Department of Energy

Agency Accession Number DA OD 4733

Prepared for

ARMY MATERIALS AND MECHANICS RESEARCH CENTER
Watertown, Massachusetts 02172

(18) (19) AMMRC TR-78-14-VOL-1

(6) # BRITTLE MATERIALS DESIGN, HIGH TEMPERATURE GAS TURBINE

Volume 1, Ceramic Component Fabrication and Demonstration

Technical Report By:

(10) Arthur F. Mclean, Ford Motor Company, Dearborn, Michigan 48121
Robert R. Baker, Ford Motor Company, Dearborn, Michigan 48121

(11) Mar[redacted]78 (12) 69 p.

(9) Interim Report No. [redacted] 12, January 1, 1977 to September 30, 1977 — 1 Jan - 30 Sep 77

Contract Number DAAG 46-71-C-0162, ARPA Order-1849

(15) Sponsored by the Defense Advanced Research Projects Agency, Department of Defense, and the Division of Transportation Energy Conservation, Department of Energy

Agency Accession Number DA OD 4733

Prepared for:

ARMY MATERIALS AND MECHANICS RESEARCH CENTER
Watertown, Massachusetts 02172

Vol 2 AD55276

141 250

ABSTRACT

In fiscal year 1977, ERDA joined forces with DARPA to support this project. The progress made on the DARPA Ceramic Turbine Testing Program is presented in this volume while the progress on the ERDA Ceramic Turbine Technology and Ceramic Turbine Materials and NDE Technology Programs is presented in Volume 2.

Duo-density rotor fabrication continued with over 600 rotor blade rings injection molded utilizing the automatic solid state control system. Yield of blade rings having no visible defects in the green, as molded, state was over 70%. Controlling the boron nitride thickness during blade fill processing coupled with a modification of the hot press graphite tooling greatly improved the hot press bonding process. The yield of flaw-free hot press bondings with these changes was 70%. This represents the most significant improvement in the yield hot press bondings to date. Finish machining of rotors continued as did non-destructive evaluation. Blade bend testing was used to monitor the quality of blade ring nitriding to insure that only the higher quality nitrided blade rings were used to fabricate rotors for testing.

Eleven duo-density ceramic turbine rotors were cold spin tested to qualify them for further hot running. Ten of the eleven reached over 50,000 rpm without failing blades, with one rotor successfully qualified to over 70,000 rpm after failing one blade at 65,640 rpm.

Development of the hot spin rigs continued. A combustor flame-out problem and a durability problem with the rotor tip shroud/failure detector were resolved. In further development of the hot spin rig, a number of ceramic and metal rotors were tested accumulating 26 hours and 68 hours respectively.

An important engine test of a duo-density silicon nitride rotor was accomplished. Rotor 1195, with the associated stationary ceramic components (nose cone, stator and tip shrouds), was successfully operated at an average Turbine Inlet Temperature (T.I.T.) of 2200°F and 45,000 rpm for 10 hours without incident. This same rotor, with 27 full length aerodynamically functional blades and stationary flowpath, was subsequently run for 25 hours at 2250°F average T.I.T. plus 1-1/2 hours at over 2500°F average T.I.T. all at 50,000 rpm. Despite a cautious shutdown a catastrophic failure occurred during the shutdown of the engine due to an overtemperatured metal component used to mount the ceramic rotor. The total hot time on the rotor was over 37 hours, all but a few minutes at a T.I.T. of 2200°F or higher, at speeds of 45,000 to 50,000 rpm, including 1-1/2 hours at 50,000 rpm and over 2500°F T.I.T. This unprecedented test is the first time a ceramic rotor has been operated at these speed/temperature/time conditions.

Fabrication development on injection molding of stators and nose cones of 2.7g/cc density was continued on a limited basis. Some additional reaction sintered silicon carbide stators were also fabricated because of promising test results previously presented. Limited development of injection molded and slip cast nose cones was continued.

Testing of stationary components continued in both qualification and durability rigs. Stators were subjected to more severe qualification tests as the vane bend load was increased from 10 to 19 pounds and the outer shroud pressure load was increased from 100 to 200 psi. Weight gains of components were monitored during hot testing at 1930 and 2500°F and found to be below previously observed values for several injection molded parts. Over 1000 hours of hot testing was accumulated on stators during this reporting period.

A complete set of silicon nitride stationary components consisting of a nose cone, two stators, two rotor tip shrouds and a second-stage stator centering ring completed the program objective of 175 hours at 1930°F plus 25 hours at 2500°F with over 40 lights. In addition, a silicon carbide stator successfully completed over 175 hours at 1930°F plus over 28 hours at 2500°F with 52 lights. Stators of two different materials, injection molded silicon nitride and reaction bonded silicon carbide, have now completed the program durability goal of 200 hours.

FOREWORD

This report is the twelfth technical report of the "Brittle Materials Design, High Temperature Gas Turbine" program initiated by the Defense Advanced Research Projects Agency, DARPA Order Number 1849, and Contract Number DAAG-46-71-C-0162. This is an incrementally-funded seven year program.

Since this is an iterative design and materials development program, design concepts and materials selection and/or properties presented in this report will probably not be those finally utilized. Thus all design and property data contained in the semi-annual reports must be considered tentative, and the reports should be considered to be illustrative of the design, materials, processing, and NDE techniques being developed for brittle materials.

In fiscal year 1977, ERDA, now Department of Energy, DOE, joined forces with DARPA to support this project. The progress made on the DARPA Ceramic Turbine Testing Program is presented in this volume while the progress on the ERDA Ceramic Turbine Technology and Ceramic Turbine Materials and NDE Technology Programs is presented in Volume 2.

The principal investigator of this program is Mr. A. F. McLean, Ford Motor Company, and the technical monitor is Dr. E. S. Wright, AMMRC. The authors would like to acknowledge the valuable contributions in the performance of this work by the following people:

Ford Motor Company

N. Arnon, R. J. Baer, J. H. Buechel, D. J. Cassidy, J. C. Caverly, G. C. DeBell, A. Ezis, E. A. Fisher, D. L. Hartsock, P. H. Havstad, J. A. Herman, R. A. Jeryan, C. F. Johnson, J. A. Mangels, W. E. Meyer, A. Paluszny, G. Peitsch, J. R. Secord, L. R. Swank, W. Trela, T. J. Whalen, R. M. Williams, W. Wu

Army Material and Mechanics Research Center

G. E. Gazza, E. M. Lenoe, R. N. Katz, D. R. Messier, H. Priest

TABLE OF CONTENTS

LIST OF ILLUSTRATIONS

LIST OF TABLES

1.0. INTRODUCTION

In July, 1971, the Defense Advanced Research Projects Agency of the Department of Defense jointly sponsored a program with Ford Motor Company to develop the use of brittle materials for engineering applications. The major program goal was to prove by a practical demonstration that efforts in ceramic design, materials, fabrication, testing and evaluation could be drawn together and developed to establish the usefulness of brittle materials in demanding high temperature structural applications.

The gas turbine engine, utilizing uncooled ceramic components in the hot flow path, was chosen as the vehicle for this demonstration. The progress of the gas turbine engine has been and continues to be closely related to the development of materials capable of withstanding the engine's environment at high operating temperature. Since the early days of the jet engine, new metals have been developed which allowed a gradual increase in operating temperatures. Today's nickel-chrome superalloys are in use, without cooling, at turbine inlet gas temperatures of 1800°F. However, there is considerable incentive to further increase turbine inlet temperature in order to improve specific air and fuel consumptions. The use of ceramics in the gas turbine engine promises to make a major step in increasing turbine inlet temperature to 2500°F. Such an engine offers significant advances in efficiency, power per unit weight, cost, exhaust emissions, materials utilization and fuel utilization. Successful application of ceramics to the gas turbine would therefore not only have military significance, but would also greatly influence our national concerns of air pollution, utilization of material resources, and the energy crisis.

At the program beginning, the application of ceramics was planned for two gas turbine engines of greatly different size. One was a small vehicular turbine of about 200 HP (contractor Ford) and the other was a large stationary turbine of about 30 MW (subcontractor Westinghouse). In the vehicular turbine project, the plan was to develop an entire ceramic hot flow path including the highly stressed turbine rotors. In the stationary turbine project, the engine was so large that plans were confined to the development of ceramic first stage vanes, and design studies of ceramic rotors.

It should be noted that both the contractor and subcontractor had in-house research programs in this area prior to initiation of this program. Silicon nitride and silicon carbide had been selected as the primary material candidates. Preliminary design concepts were in existence and, in the case of the vehicular engine, hardware had been built and testing had been initiated.

One difference in philosophy between the two projects is worth noting. Because the ceramic materials, fabrication processes, and designs were not developed, the vehicular turbine engine was designed as an experimental unit and featured ease of replacement of ceramic components. Iterative developments in a component's ceramic material, process, or design can therefore be engine-evaluated fairly rapidly. This work can then parallel and augment the time-consuming efforts on material and component characterization, stress analysis, heat transfer analysis, etc. Some risk of damage to other components is present when following this approach, but this is considered out-weighed by the more rapid acquisition of actual test information. On the other hand, the stationary turbine engine is so large, so expensive to test, and contains such costly and long lead-time components which could be damaged or lost by premature failure, that very careful material and design work must be performed to minimize the possibility of expensive, time-consuming failures during rig testing and, even more critically, during engine testing. These anticipated difficulties in applying ceramics to a large stationary turbine engine were substantiated to the extent that the scope of work for the stationary turbine project was revised to demonstrate ceramic stator vanes in a static test rig rather than the formidable task of testing in an actual 30 MW test turbine engine[8]. The stationary turbine project was completed in 1976 with the testing of ceramic stator vanes in a static test rig for 100 cycles up to temperatures of 2500°F. The Westinghouse final reports on the stationary turbine project have been compiled and are nearing publication[12]. This report and future reports under this contract will therefore deal entirely with the vehicular turbine project.

The principal objective of the Vehicular Turbine Project was to develop ceramic components and demonstrate them in a 200-HP size high temperature vehicular gas turbine engine. The entire hot flow path will comprise uncooled parts. The attainment of this objective will be demonstrated by 200 hours

of operation over a representative duty cycle at turbine inlet temperatures of up to 2500°F. Successful completion of this program objective will not only demonstrate that ceramics are viable structural engineering materials, but will also represent a significant breakthrough by removing the temperature barrier which has for so long held back more widespread use of the small gas turbine engine.

Development of the small vehicular regenerative gas turbine engine using superalloy materials has been motivated by its potentially superior characteristics when compared with the piston engine. These include:

— Continuous combustion with inherently low exhaust emissions

— Multi-fuel capability

— Simple machine,— fewer moving parts

— Potentially very reliable and durable

— Low maintenance

— Smooth, vibration-free production of power

— Low oil consumption

— Good cold starting capabilities

— Rapid warm-up time

With such impressive potential, the gas turbine engine using superalloys has been under investigation by every major on-highway and off-highway vehicle manufacturer in the world, and, in November 1976, was selected by the U.S. Army as the engine for the XM1 tank.

In addition, the small gas turbine engine without exhaust heat recovery (i.e., non-regenerative) is an existing proven type of power plant widely used for auxiliary power generation, emergency standby and continuous power for generator sets, pump and compressor drives, air supply units, industrial power plants, aircraft turboprops, helicopter engines, aircraft jet engines, marine engines, small portable power plants, total energy systems, and hydrofoil craft engines. While this variety of applications of the small gas turbine using superalloys is impressive, more widespread use of this type engine has been hampered by two major barriers, efficiency and cost. This is particularly so in the case of high volume automotive applications.

Since the gas turbine is a heat engine, efficiency is directly related to cycle temperature. In current small gas turbines, maximum temperature is limited not by combustion, which at stoichiometric fuel/air ratios could produce temperatures well in excess of 3500°F, but by the capabilities of the hot component materials. Today, nickel-chrome superalloys are used in small gas turbines where blade cooling is impractical, and this limits maximum turbine inlet gas temperature to about 1800°F. At this temperature limit, and considering state-of-the art component efficiencies, the potential overall efficiency of the small regenerative gas turbine is not significantly better than that of the gasoline engine and not as good as the Diesel. On the other hand a ceramic gas turbine engine operating at 2500°F will have fuel economies superior to the conventional Diesel at significant weight savings.

The other major barrier is cost and this too is strongly related to the hot component materials. Nickel-chrome superalloys, and more significantly cobalt based superalloys which meet typical turbine engine specifications, contain strategic materials not found in this country and cost well over $5/lb. This is an excessive cost with respect to high volume applications such as trucks or automobiles.

High temperature ceramics such as silicon nitride or silicon carbide, on the other hand, are made from readily available and vastly abundant raw materials and show promise of significantly reduced cost compared to superalloys, probably by at least an order of magnitude.

Thus, successful application of ceramics to the small turbine engine, with an associated quantum jump to 2500°F would not only offer all of the attributes listed earlier, but in addition would offer superior fuel economy and less weight at competitive cost with the piston engine.

The vehicular project is organized to design and develop an entire ceramic hot flow path for a high temperature, vehicular gas turbine engine. Figure 1.1 shows a schematic of this experimental regenerative engine, designated model 820. Air is induced through an intake silencer and filter into a radial compressor, and then is compressed and ducted through one side of each of two rotary regenerators. The hot compressed air is then supplied to a combustion chamber where fuel is added and combustion takes place.

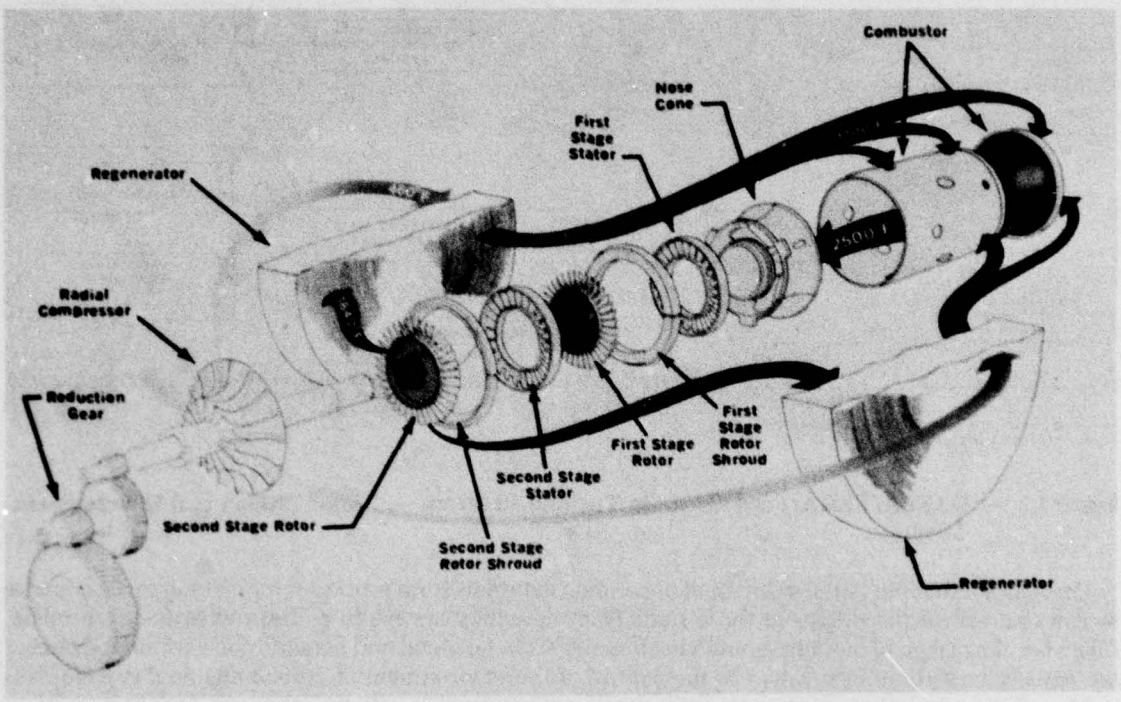

Figure 1.1 — Schematic View of the Vehicular Turbine Engine Flowpath

The hot gas discharging from the combustor is then directed into the turbine stages by a turbine inlet nose cone. The gas then passes through the turbine stages which comprise two turbine stators, each having stationary airfoil blades which direct the gas onto each corresponding turbine rotor. In passing through the turbine, the gas expands and generates work to drive the compressor and supply useful power. The expanded turbine exhaust gas is then ducted through the hot side of each of the two regenerators which, to conserve fuel, transfer much of the exhaust heat back into the compressed air.

The hot flow path components, subject to peak cycle temperature and made out of superalloys in today's gas turbine, are the combustor, the turbine inlet nose cone, the turbine stators, the turbine tip shrouds, and the turbine rotors. These are the areas where the use of ceramics could result in the greatest benefits, therefore these components have been selected for application of ceramics in the vehicular turbine project.

Successful development of the entire ceramic flow path, as demonstrated in a high temperature vehicular gas turbine engine, will involve a complex iterative development. Figure 1.2 shows a block diagram flow chart, including the feedback loops, of the major factors involved, and serves to illustrate the magnitude of this complex and comprehensive iterative development program. Of particular importance is the interrelationship of design, materials development, ceramic processes, component rig testing, engine testing, non-destructive evaluation and failure analysis.

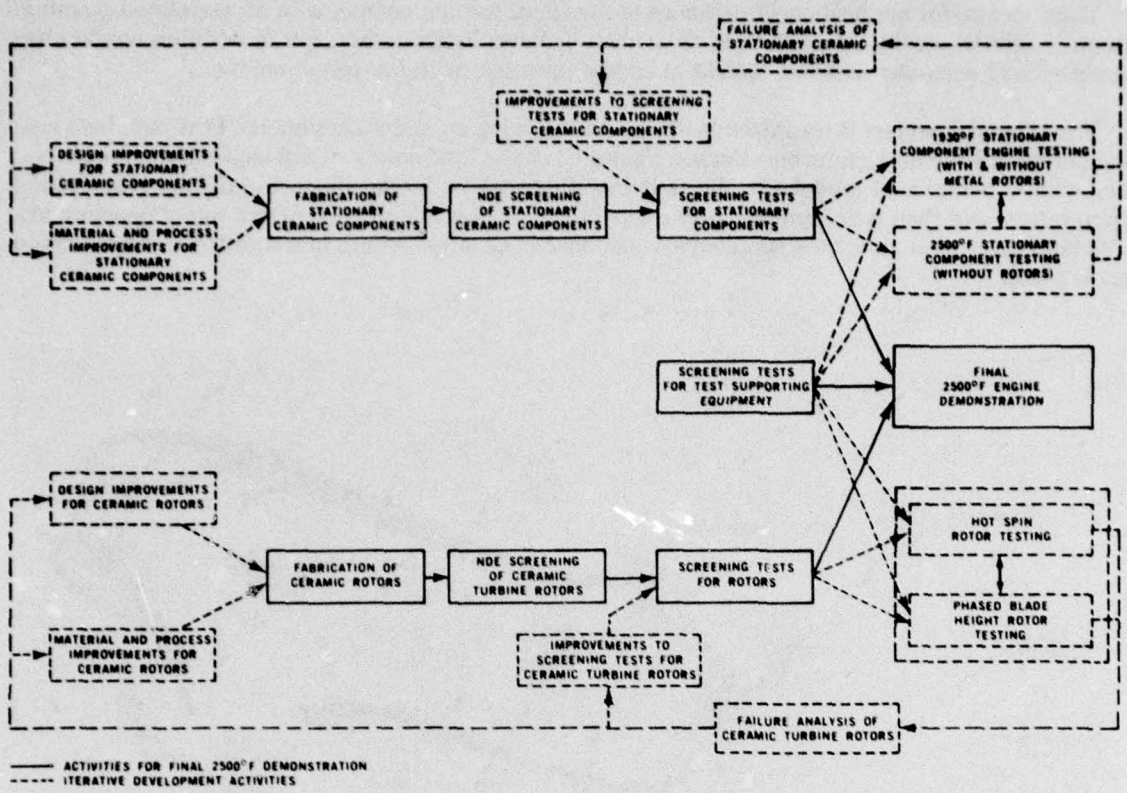

Figure 1.2 — DARPA/ERDA/Ford Ceramic Turbine Program — Major Project and Development Loops

One cannot divorce the development of ceramic materials from processes for making parts; no more so can one isolate the design of those parts from how they are made or from what they are made. Likewise, the design of mountings and attachments between metal and ceramic parts within the engine are equally important. Innovation in the control of the environment of critical engine components is another link in the chain. Each of these factors has a relationship with the others, and to obtain success in any one may involve compromises in the others.

Testing plays an important role during the iterative development since it provides a positive, objective way of evaluating the various combinations of factors involved. If successful, the test yields the credibility to move on to the next link in the development chain. If unsuccessful, the test flags a warning and prompts feedback to earlier developments to seek out and solve the problem which has resulted in failure. Finally, all of the links in the chain are evaluated by a complete engine test, by which means the ultimate objective of the program will be demonstrated. It is important then to recognize that this is a systems development program — no single area is independent, but each one feeds into the total iterative system.

In fiscal year 1977, ERDA joined forces with DARPA to support the program. The ERDA Division of Transportation, working closely with NASA-Lewis, have been supporting process development to improve the fabrication of ceramic turbine rotors, and ERDA's Division of Conservation Research and Technology has been supporting some of the work on non-destructive evaluation of ceramics and ceramic materials characterization (Figure 1.3). AMMRC has maintained overall participative monitoring responsibility for this joint program.

Volume 1 of this report covers the DARPA Ceramic Turbine Testing Program and represents the 12th report of progress. Volume 2 covers the progress on ERDA's Ceramic Turbine Rotor Technology and Ceramic Turbine Materials and NDE Technology Programs.

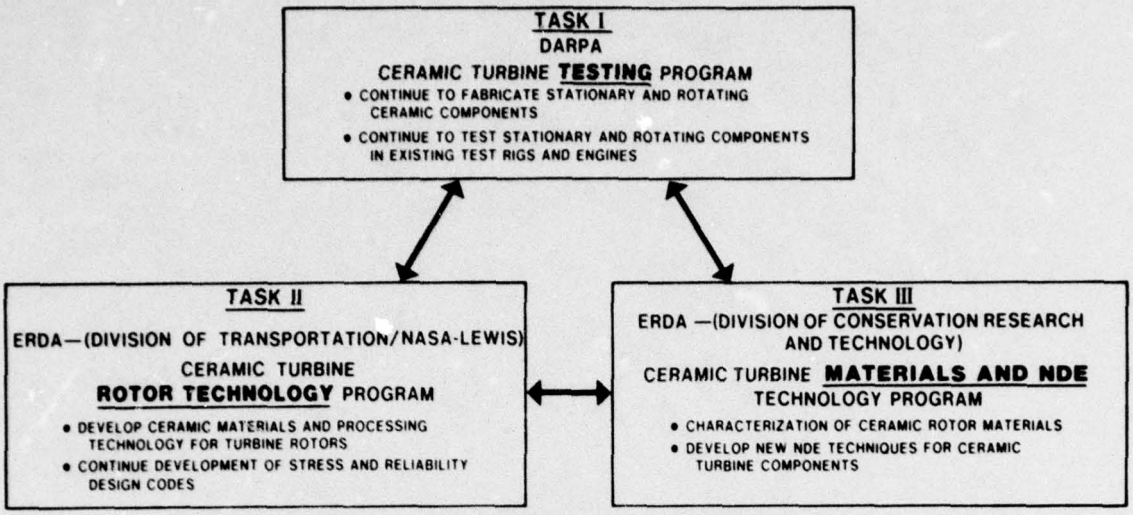

Figure 1.3 — DARPA/ERDA Supported Tasks in the "Brittle Materials Design, High Temperature Gas Turbine" Program

The Ford/DARPA Ceramic Turbine Testing Program represents a continuation of the FORD/ARPA "Brittle Materials Design, High Temperature Gas Turbine" Program [1-11]. DARPA's goal remains to show, by a 200 hour demonstration (at temperatures up to 2500°F) of a ceramic gas turbine engine, that ceramic design, materials, fabrication, testing and evaluation can be sufficiently developed to establish the usefulness of brittle materials for demanding engineering applications. During the past nine months, the DARPA portion of the program was specifically oriented toward the evaluation of the reliability of state-of-the-art ceramic components which were developed over the previous five and one half years.

Since the beginning of the FORD/DARPA program, a considerable amount of technology has been developed and applied to the design and analysis of ceramic components. Similar progress was made on ceramic material and process development, and on ceramic component and engine testing. During this reporting period, these technologies were used to fabricate stationary and rotating ceramic components and assess their reliability by testing in rigs and engines.

Fabrication of ceramic turbine rotors, stators, nose cones, rotor tip shrouds, combustors, and regenerator cores and seals was continued in order to supply components for test rig and engine evaluation. In the case of ceramic rotors for testing, rotor fabrication incorporated, wherever possible, process improvements developed under the Ceramic Turbine Rotor Technology Program supported by ERDA Division of Transportation (Volume 2 of this report). The components were prepared for testing through several inspection stages, including close visual inspection (10-70X), X-ray radiography and die penetrant inspection where applicable, both before and after machining.

Test and evaluation of ceramic turbine components included screening and qualification tests previously developed to eliminate weak or flawed parts. Stationary ceramic components were durability tested in static test rigs and in the full engine configuration. Ceramic turbine rotors were evaluated in a modified 820 ceramic gas turbine engine.

2.0 SUMMARY

2.1 PROGRAM HIGHLIGHTS

This section presents a brief listing of major accomplishments achieved in the Ford/DARPA/-ERDA program. The numbers in parentheses refer to references listed in Section 4.0 of this report.

- injection molding and slip casting technology was developed to fabricate complex shaped silicon preforms such as blade rings, stators and nose cones which nitride to 2.7g/cc [9,10,11].
- solid state control system designed, built and used to regulate the molding parameters and automate the fabrication of blade rings, stators and nose cones[11].
- nitrogen/hydrogen demand cycle conceived and implemented for nitriding silicon compacts to a density of 2.55-2.7g/cc[9].
- 2.7g/cc injection molded reaction sintered silicon nitride achieved 4 pt bend strengths of 43 ksi at 70°F[8] and no time dependent failures at 20-30 ksi and 1900-2000°F for up to 200 hours[10].
- many rotor fabrication approaches investigated and discarded or shelved[1-5]. Duo-density silicon nitride rotor concept conceived[2] consisting of reaction bonded silicon nitride blades and a hub of hot pressed silicon nitride.
- hot press bonding technology was developed to produce a 70% yield of duo-density rotors free of flaws induced by hot pressing[12].
- processes for making all ceramic (silicon nitride and/or silicon carbide) parts (combustor, nose cone, stators, rotor tip shrouds and rotors) devised and developed. Many parts of each type made to develop the processes and evaluated by testing[1-11].
- ultrasonic C-scan, acoustic emissions and microfocus X-ray techniques investigated for NDE of ceramic components [1-6,11].
- rotor blade and stator vane bend tests, stator shroud test and 10-light qualification tests developed as screening tests for ceramic components[6,8-11].
- 2.7g/cc stator vanes survived over 9000 cycles to 2700°F on the Thermal Shock Rig [8].
- a probabilistic design technique for ceramics was developed and applied to ceramic rotors[5].
- hot pressed Si_3N_4 rotor hubs demonstrated a characteristic failure speed of 108,500 rpm with a Weibull slope of 14.8 which was in agreement with analytical predictions[10].
- aerodynamic/reliability studies showed a 3-stage turbine at 50,000 rpm had a higher reliability than a 2-stage at 64,000 rpm for the same power and efficiency[11].
- **all stationary ceramic components successfully met the program durability goal*.**

	Hours at 1930°F		Hours at 2500°F		Total Hours
Program Goal	**175**	**+**	**25**	**=**	**200**
Reaction Bonded SiC Combustor	175		26		201
Reaction Sintered Si_3N_4 Nose cone	175		26		201
Reaction Sintered Si_3N_4 Stators	175		26		201
Reaction Bonded SiC Stator	176		29		205
Reaction Sintered Si_3N_4 Shrouds	175		26		201

NOTE: Refer to this report for items noted*.

- duo-density silicon nitride rotor #1195 engine tested for 10 hours at 2200°F Turbine Inlet Temperature and 45,000 rpm without failure; rotor additionally tested, successfully, for 25 hours at 2250°F, 50,000 rpm, plus 1½ hours at 2500°F, 50,000 rpm; failure occurred during a shutdown due to 790°F overtemperature in the vicinity of the curvic coupling*.

2.2 CUMULATIVE PROGRAM SUMMARY

To meet the program objectives, the work has been divided into two major tasks:

1. Ceramic Component Development

2. Materials Technology

A review of progress throughout the history of this program and present status in each of these tasks is summarized in Section 2.2.1 and 2.2.2.

2.2.1 CERAMIC COMPONENT DEVELOPMENT

Two categories of ceramic components are under development: rotating parts (i.e., ceramic rotors), and stationary parts (i.e., ceramic stators, rotor tip shrouds, nose cones, and combustors). In this iterative development, each component will pass through various phases comprising design and analysis, materials and fabrication, and testing.

CERAMIC ROTORS

The development of the ceramic turbine rotors is by far the most difficult task in the ARPA program. This is because of:

- The very complex shape of the turbine rotor forcing the development of new and unique fabrication capabilities.
- The high centrifugal stresses associated with high maximum rotor speeds.
- The high thermal stresses and associated thermal fatigue resulting from both steady state and transient high temperature gradients from the rotor rim to the rotor hub.
- The hostile environment associated with the products of combustion from the combustor.
- The high temperature of the uncooled blades resulting from turbine inlet gas temperatures of 2500°F.

Progress and Status

- Fully dense Si_3N_4 first and second stage integral rotors were designed and analyzed (1,2,3,4).
- A method of attaching rotors was conceived and designed (1,2).
- The following approaches for making integral rotors were investigated but discontinued:

— Direct hot pressing of an integral Si_3N_4 rotor (1).

— Ultrasonic machining of a rotor from a hot pressed Si_3N_4 billet (1,2,3).

— Hot pressing an assembly of individually hot pressed Si_3N_4 blades (1,2).

— Pseudo-isostatic hot pressing of an injection molded Si_3N_4 preform (1,2,3).

— Hot pressing using comformable tooling of preformed Si_3N_4 blades and hub (2,3,4).

— Fabrication of a dense SiC blade ring by chemical vapor desposition (1,2,3,4).

— Electric discharge machining of a rotor from a hot pressed SiC billet (2,3,4).

- A "duo-density" Si_3N_4 ceramic rotor was conceived and designed (3).

- Tooling to injection mold Si_3N_4 blade rings was designed and procured (3).

- Several hundred hot press bonding of duo-density rotors have been carried out (10). These have progressed from rotors with flat-sided hubs to fully-contoured hubs made simultaneously with the hot press bonding operation. Prior severe blade ring distortion problems have been solved by using a double blade fill to support the blade ring during bonding. In addition, the diffusion bond has been improved as evidenced by microstructural examination. Experiments were conducted using magnesium nitrate instead of magnesium oxide as a densification aid. Excellent bonding and density were achieved but strength was deficient. Successful modifications were made to the graphite wedge system to reduce blade ring cracking and tearing problems. Problems which remain are occasional blade ring and rim cracking (4,5,6,7,8).

- Over 110 cold spin tests resulted in blade failures over a range of speeds, some of which exceeded full speed requirements of the new Design D′ blading. However, an improvement in consistency is required if a reasonable yield from the blade ring fabrication process is to be achieved. This emphasizes the need for three-dimensional blade stress analysis as well as development of a higher strength, better quality blade material. Cold spin testing of rotor hubs of hot pressed Si_3N_4 showed a characteristic failure speed of 115,965 rpm with a Weibull rpm slope of 17.66 (7). Several hot pressed hubs, made by the hot press bonding process, were cold spun to destruction, and showed results consistent with hot pressed hubs fabricated separately (8). A high speed motion picture study (3000 frames/sec) was conducted of a turbine rotor failure in the cold spin pit (8).

- A three dimensional model of the rotor blade along with heat transfer coefficients has been generated for thermal and stress analysis (5,6,8).

- Development of better quality blade rings continues. X-ray radiography of green parts has proved effective in detecting major flaws. Slip cast Si_3N_4 test bars having a density of 2.7 gm/cc show four point MOR of 40,000 psi. Processes to slip cast a rotor blade ring have been investigated as have methods of achieving 2.7 gm/cc density with injection molded material (6,7,8).

- Thermal shock testing simulating the engine light-off condition was conducted on rotor blade rings for approximately 2,500 cycles without damage (5,6).

- A technique to evaluate probability of failure using Weibull's theories was developed and applied to ceramic rotors (5).

- A test rig was designed and built to simulate the engine for hot spin testing of ceramic rotors (3,4,5). A set of low quality duo-density rotors was spin tested to 20% speed and 1950°F for a short time before failure, believed due to an axial rub (7).

- A revised rotor design (Design D) was conceived, using common rotors at first and second stage locations (7).

- A lower stress version of the Design D rotor, designated Design D′, has been designed using radially stacked blade sections. Blade centrifugal stresses were reduced from 21,000 psi in Design D to 13,180 psi in Design D′ (8).

- The rotor test rig was rebuilt and testing initiated to evaluate the rotor attachment mechanism and the curvic coupling mounting design. Hot-pressed Si_3N_4 rotor hubs were subjected to 10 operating cycles from 900 to 1950°F, during a 3-3/4 hour test, without damage (8).

- Design codes for ceramics were refined to include nonlinear thermal properties of materials and to allow for the specification of the MOR-strength and Weibull "m" requirements for a given failure at a specified loading and reliability level (9,10).

- Rotor hubs were successfully densified and press bonded at both 2% and 3-1/2% MgO levels, resulting in reduction of MgO migration into the blade ring and improved high temperature strength over previous pressings with 5% MgO (9).

- A design C duo-density rotor with a few obviously flawed blades removed was cold spin tested after static oxidation at 1900°F for 200 hours. A single half-blade failure occurred at 53,710 rpm, which corrects to 68,000 rpm or 105% speed for the present shorter bladed Design D′ configuration. The results of a number of spin tests of slip cast Si_3N_4 blade segments were combined to yield a median failure speed of 64,000 rpm (9).

- Over five hundred blade rings, previous to Design D′, were injection molded for press bonding experiments, cold spin tests, and hot tests (9).

- New tooling to injection mold the lower stressed Design D′ rotor blade rings was received and trial moldings to establish molding parameters were initiated (9).

- Progress has been made in several aspects of the press-bonding step of duo-density rotor fabrication. A problem of excessive deflection of the graphite support structure beneath the rotor assembly, permitting bending and subsequent blade fracture, was solved by the substitution of high modulus hot pressed SiC for the low modulus graphite. Increasing the rate of pressure application also improved the quality of the hub sections (9).

- A new hot spin test rig, designed to improve the turn-around-time in testing turbine rotors, has been constructed, and is currently in the shakedown testing phase. Using gas burners instead of a gas turbine combustion system, this rig simulates the engine environment and was designed to be quickly rebuilt following rotor failures (9).

- In a program to engine evaluate ceramic rotors having reduced blade length (and less risk of catastrophic failure), two duo-density Si_3N_4 rotors with the blades shortened to 10% of the design length were selected and cold spun to 64,000 rpm (9). These rotors were then hot tested in an engine for 45 minutes at 32,000 rpm and 2000°F turbine inlet temperature without failure (10).

- The aerodynamic design of an increased efficiency turbine, designated Design E, was initiated. Flowpath optimization, a one dimensional stress analysis, and preliminary detailed blade section definition were completed for both the first and second stage turbine stators and rotors (9).

- A process has been developed to slip cast turbine rotor blade rings (9).

- 3-D stress and reliability analyses were performed on preliminary blade configurations for the increased efficiency Design E turbine rotors (10).

- 500 Design D′ blade rings have been injection molded which will nitride to 2.7 g/cc density (10).

- A new fabrication approach, called the 3 piece concept, to make duo-density silicon nitride turbine rotors, was conceived and demonstrated that a significant reduction of applied loads during hot press bonding could be achieved, generally eliminating blade and rim cracking (10).

- Good correlation was demonstrated between predicted cold burst speed and actual spin test results on nine rotor hubs spun to destruction (10).

- Six available duo-density turbine rotors of imperfect quality were used to check out the hot spin rigs by hot spin testing to failure, with failure speeds ranging from 12,000 rpm to 35,300 rpm at rotor rim temperatures ranging from 1780° to 2250°F, (corresponding to equivalent estimated blade tip temperatures in an engine of 1930°F to 2400°F) (10).

- A duo-density rotor with flawed blades removed achieved 52,800 rpm in the modified design engine with ceramic stationary flowpath prior to an unscheduled dynamometer shutdown. A maximum turbine inlet temperature of 2650°F was observed during this run. Post inspection showed all

ceramic parts to be crack free. The rotor failed during a subsequent run at 50,000 rpm and 2300°F T.I.T. (10).

- Since the Weibuil probabilistic method is being used in the design of ceramic turbine rotors, an investigation of various estimation techniques to obtain Weibull parameters from test data was carried out. The method selected and used in this program is the "Maximum Likelihood Estimator" (MLE) method. Confidence intervals in estimating Weibull parameters using the MLE method were computed to vary significantly with the number of samples tested (11).

- An analytical method was prepared, based on the Wiederhorn-Evans approach (11), to predict the time-to-failure of complex, multiaxially-stressed ceramic components such as the ceramic turbine rotor (11).

- Effort to design improved efficiency ceramic turbine stages (Design E) led to the consideration of a 3-stage turbine versus the current 2-stage design. It was shown that, for the same overall level of efficiency, a three stage turbine would have a significantly higher reliability and could operate at 50,000 rpm maximum speed rather than the 64,000 rpm required to obtain the same power output from a two stage turbine. Alternately, for equal levels of overall reliability, the 3-stage design can be expected to be 3-5 percentage points better in aerodynamic efficiency. Further work on improved efficiency Design E turbine stages was terminated as a result of reductions in the overall program (11).

- An automatic control system utilizing solid state logic elements was designed, built and applied to the injection molding of ceramic turbine components, particularly rotor blade rings. The objective was to consistently control such parameters as molding material temperature, die temperature and various sequencing times. The desired setting of each parameter was varied systematically to optimize the molding process for rotor blade rings based on visual and X-ray inspection. In addition to using optimized molding parameters, it was found necessary to clamp the die accurately to avoid blade root cracks, and to pre-extrude the starting material to avoid unmelted inclusions. A quantity of Design D′ rotor blade rings was molded in the 2.7 g/cc density Si_3N_4 material system utilizing these improvements for subsequent processing (11).

- A parametric study of processing hot pressed Si_3N_4 (HPSN) involving Si_3N_4 powder quality, hot pressing additive, powder milling conditions, and hot pressing conditions, was initiated in an effort to improve the expected reliability of duo-density Si_3N_4 turbine rotors. Sixty HPSN billets were made and used to establish Weibull strength data at 1600°F and 2200°F which is representative of the maximum operating temperatures at the rotor bore and bond respectively (11).

- Test bars cut from three-piece duo-density Si_3N_4 rotors showed low strength in the bond between the HPSN hub and the HPSN bonding ring. Failures of this bond in spin tests also confirmed its lack of strength. In parallel, parametric studies on hot pressing Si_3N_4 showed that flat sided HPSN discs could be made at pressures as low as 500 psi. As a result, an improved two-piece, duo-density Si_3N_4 rotor with a simplified hub profile was considered; this would eliminate the troublesome hub/bonding ring bond and facilitate low hot pressing pressures which should minimize blade ring damage. Ten such two-piece, duo-density Si_3N_4 rotors were hot press bonded at pressures from 500 to 1500 psi using a 3-1/2 w/o MgO additive material for the hub. Three of these had no rim cracks and only minor blade cracking, and have been selected for finish machining and subsequent spin testing (11).

- Development of the hot spin rig continued and resulted in improvements in the failure detector system, temperature measuring system, and burst absorption capability. To check out the latter, a bladeless rotor was accelerated to 64,840 rpm and the temperature gradient increased until failure occurred. The attachment bolt fractured as designed, the ceramic fiber insulation and stainless steel backing absorbed the failure, and the rotor shaft was only slightly scored at the bearing journal. This damage was quickly repaired to demonstrate a relatively fast turn-around time (11).

- Finite element models of a duo-density Si_3N_4 rotor tested in the hot spin rig were made and will be used to calculate temperatures and stresses in the rotor for a given operating speed and rim temperature (11).

- A number of lubricants have been investigated for the rotor ceramic-to-metal curvic coupling including Nickel Ease, Molykote, Electrofilm, Borkote, and Molydisulfide. A problem of limited life at the 1400°F operating temperature resulted in the development of a 1/4 mil thick gold coating on the contacting surfaces of the curvic teeth. Such a coupling has been tested through four complete thermal cycles with no significant deterioration, and will be used in the next engine test of a ceramic rotor (11).

- Controlling the boron nitride thickness during blade fill processing coupled with a modification of the hot press graphite tooling greatly improved the hot press bonding process increasing the yield of flaw free hot press bondings to 70%. This represents the most significant improvement in the yield of hot press bondings to date *.

- Surface and internal flaws were found in most injection molded reaction sintered silicon nitride blade rings by visual and destructive evaluation *.

- Ten of eleven duo-density silicon nitride turbine rotors were cold spun to over 50,000 rpm without *failing blades — one rotor successfully* qualified to over 70,000 rpm after failing one blade at 65,640 rpm *.

- Seven ceramic rotors were tested in the hot spin rigs accumulating over 26 hours of hot testing. Rotor 1256 operated at 1800°F rim temperature at 50,000 rpm for 18 hours and 42 minutes before failure *.

- Duo-density rotor 1195 was engine tested for 10 hours at 2200°F Turbine Inlet Temperature and 45,000 rpm without failure; rotor additionally tested, successfully, for 25 hours at 2250°F, 50,000 rpm plus 1½ hours at 2500°F, 50,000 rpm, failure occurred during shutdown *.

CERAMIC STATORS, ROTOR SHROUDS, NOSE CONES, AND COMBUSTORS

While development of the ceramic turbine rotor is the most difficult task, development of the stationary ceramic flow path components is also vitally necessary to meet the objective of running an uncooled 2500°F vehicular turbine engine. In addition, success in designing, fabricating, and testing these ceramic components will have an important impact on the many current applications of the small gas turbine where the use of stationary ceramics alone can be extremely beneficial. The progress and status of these developments is summarized, taking each component in turn.

Progress and Status

Ceramic Stator

- Early Design A first stage stators incorporating the turbine tip shrouds had been designed, made by assembling individual injection molded reaction bonded Si_3N_4 vanes, and tested, revealing short time thermal stress vane failures at the vane root (1).

- Investigation of a number of modified designs led to Design B, with the rotor shroud separated from the stator. Short time thermal stress vane failures at the vane root were eliminated (1).

- In the fabrication of stators, the starting silicon powder, the molding mixture, and the nitriding cycle were optimized for 2.2 gm/cc density reaction bonded Si_3N_4 (2,3).

- Engine and thermal shock testing of first stage Design B stators revealed a longer term vane cracking problem at the vane mid-span. This led to modification of the vane chord, designated the Design C configuration, which solved the vane mid-span cracking problem (3).

- A remaining problem in first and second stage Design B stators was cracking of outer shrouds, believed due to the notch effect between adjacent vanes. To solve this, a one-piece first stage stator (Design C) was designed and tooling was procured (4,5).

- The Design B second stage stator could not be made in one piece due to vane overlap, so an "inverted channel" design was investigated to eliminate notches at the outer diameter. However, engine testing showed that axial cracking of the outer shroud remained a problem (3,4,5,6).

- A 50 hour duty-cycle engine test of the hot flow path components to 1930°F was completed. The assembled first stage Design C stator was in excellent condition; 8 out of 33 vanes in the second stage inverted channel stator had developed fine cracks (6).

- A 100 hour duty-cycle engine test of the hot flow path components (without a second stage stator) to 1930°F was completed. The reaction bonded silicon nitride (2.55 g/cc density) one piece first stage Design C stator successfully survived this test (7).

- Improvements in materials and processing resulted in the fabrication of flaw free one piece stators of 2.55 gm/cc density (8).

- A test was devised for mechanically loading stator vanes to failure which provided useful information for material and process development (8).

- Thermal shock testing of 2.7 gm/cc density stator vanes revealed no detectable cracking and negligible strength degradation after 9000 cycles of heating to 2700°F and cooling in the thermal shock rig (8).

- Processing of 2.55 gm/cc density injection molded stators continued. Consistently high weight gains (61-62%) have been obtained using the Brew all-metal furnace employing a slow, gradual rate-of-rise cycle, 4% H_2-96% N_2 gas under static pressure, and Si_3N_4 setters and muffles (9).

- An injection molded stator of 2.55 gm/cc density Si_3N_4 survived static testing (no rotors) for 175 hours at 1930°F steady state. Weight gain of the stator was less than 1%, and this stabilized after 10 hours of testing. The stator is in excellent condition (9).

- Testing of stators up to 2500°F in the Flow Path Qualification Test Rig was initiated with over eight hours of testing accumulated at 2500°F (9).

- A reaction bonded silicon carbide stator successfully accumulated 147 hours of testing at 1930°F and remains crack free (10).

- Over nine hours of testing of a silicon nitride stator were accumulated without incident in the modified engine configuration to a maximum turbine inlet temperature of 2650°F (10).

- As a result of funding reductions in the overall program, a short-term attempt to fabricate stationary ceramic components was made and the best available parts were selected for testing. Attempts to injection mold one-piece stators in the 2.7 g/cc density Si_3N_4 material system were made and a variety of molding parameters were examined. A number of stators were processed with good vane quality but questionable outer shroud quality (11).

- Three 2.7 g/cc density Si_3N_4 stators passed mechanical loading tests in the stator vane and outer shroud loading fixtures though one was categorized poor due to visual fillet cracks. This latter one failed the 10-light qualification test. The other two stators passed the 10-light qualification test (11).

- A review was made of earlier durability testing of 2.55 g/cc density Si_3N_4 stators at 1930°F. The weight gain was a measure of incipient failure. For example, the failures of six 2.55 g/cc density Si_3N_4 stators were associated with weight gains in excess of 1.9%. This wide variation of weight gain is thought to be due to the variation in open porosity caused during the nitriding cycle. It is expected that this problem will be considerably lessened for higher density 2.7 g/cc density Si_3N_4 having good quality microstructure (11).

- Over 1000 hours of hot testing was accumulated on ceramic stators during this reporting period*.

- Ceramic stators of two different materials, injection molded reaction bonded silicon nitride and reaction bonded silicon carbide, have now successfully completed the program durability goal of 200 hours *.

Ceramic Rotor Shrouds

- Separate first and second stage ceramic rotor shrouds, which are essentially split rings, evolved in the stator change from Design A to Design B (1).

- As a result of rig and engine testing, rotor shrouds made of cold pressed, reaction sintered Si_3N_4 were modified to have flat rather than conical side faces (2).

- Because of occasional cracking, cold pressing was replaced with slip casting for making higher density rotor shrouds, resulting in a 2-3 fold increase in strength (3).

- Slip casting of rotor shrouds solved the cracking problem but revealed a dimensional change problem as a function of operating time. This was solved by incorporation of nitriding aids, heat treatment cycles, and other changes in the fabrication process which reduced instability to acceptable levels (4,5,6).

- A 50 hour duty cycle engine test of the hot flow path components to 1930°F was completed, after which both first and second stage rotor shrouds were in excellent condition (6).

- A 100 hour duty cycle engine test of the hot flow path components to 1930°F was completed, after which both first and second stage rotor shrouds were in excellent condition (7).

- Further testing of rotor shrouds to 245 hours and over 100 lights showed them to remain crack free and in excellent condition (7).

- Over nine hours of testing slip cast Si_3N_4 rotor tip shrouds were accumulated without incident in the modified engine configuration used for testing a ceramic turbine rotor up to a maximum turbine inlet temperature of 2650°F (11).

- Both ceramic first and second stage rotor tip shrouds successfully completed the program durability goal of 200 hours *.

Ceramic Combustors

- Slip cast silicon nitride and various grades of recrystalized silicon carbide (crystar) were eliminated as ceramic combustor materials(4).

- A thick-walled, reaction bonded silicon carbide (REFEL) combustor successfully completed the 200 hour duty cycle test. A total of 26 hours and 40 minutes was accumulated at a turbine inlet temperature of 2500°F (10). This combustor was also successfully tested in an engine (8).

- Three thin-walled, reaction bonded silicon carbide (REFEL) combustors were successfully qualified over a 10 hour portion of the ARPA duty cycle (10).

Ceramic Nose Cones

- Early Design A nose cones had been designed, made from injection molded reaction sintered Si_3N_4, and tested (1).

- The nose cone was modified to Design B to accommodate the Design B first stage stator. Several Design B nose cones were made and tested in rigs and engines (2).

- Voids in molding nose cones were minimized by preferentially heating the tooling during molding (5).

- Circumferential cracking and axial cracking problems led to pre-slotted, scalloped nose cones designated Design C (3,4,5,6).

- A 50 hour duty cycle engine test of the hot flow path components to 1930°F was completed, after which the Design C nose cone was in excellent condition (7).

- A 100 hour duty cycle engine test of the hot flow path components to 1930°F was completed, after which the Design C nose cone was in excellent condition (7).

- Further testing of the 2.2 g/cc density nose cone to 221 hours showed it to remain crack free and in excellent condition (7).

- Improvements in materials and processing resulted in the fabrication of flaw free nose cones of 2.55 gm/cc density (8).

- Processing of 2.55 gm/cc density injection molded nose cones continued. Consistently high weight gains (61-62%) have been obtained using the Brew all-metal furnace employing a slow, gradual rate-of-rise cycle, 4% H_2-96% N_2 gas under static pressure, and Si_3N_4 setters and muffles (9).

- Testing of nose cones up to 2500°F in the Flow Path Qualification Test Rig was initiated with over eight hours of testing accumulated at 2500°F (9).

- Over nine hours of testing a silicon nitride nose cone were accumulated without incident in the modified engine configuration to a maximum turbine inlet temperature of 2650°F (10).

- As a result of funding reductions in the overall program, a short-term attempt to fabricate stationary ceramic components was made and the best available parts were selected for testing. A number of Design D nose cones were injection molded in the 2.7 g/cc density Si_3N_4 material system using an automated molding control system, primarily developed to make high quality rotor blade rings. Nose cones were processed through nitriding and appeared visually good except for fine cracks between the strut and inner nose (11).

- Three 2.7 g/cc density Si_3N_4 nose cones successfully passed the 10-light qualification test. One of these has accumulated 10 hours of testing at 1930°F (11).

- A slip cast silicon nitride nose cone was fabricated and tested at 1930°F.

- An injection molded reaction bonded silicon nitride nose cone successfully completed the program durability goal of 200 hours *.

2.2.2 MATERIALS TECHNOLOGY

Materials technology forms the basis for component development including component design, component fabrication, material quality in the component as-made, and evaluation by testing. There are three major categories under materials technology — materials engineering data, materials science, and non-destructive evaluation. Progress and present status in each of these areas is summarized below:

Materials Engineering Data

- Techniques were developed and applied for correlating the strength of simple ceramic spin disks with bend test specimens using Weibull probability theories (5).

- Elastic property data as a function of temperature was determined for various grades of silicon nitride and silicon carbide (2,3,4,5,6,7,9).

- The flexural strength vs. temperature of several grades of SiC and Si_3N_4 was determined (3,4,5,6,9,10).

- The compressive strength vs. temperature of hot pressed SiC and hot pressed Si_3N_4 was determined (4).

- Creep in bending at several conditions of stress and temperature was determined for various grades of reaction sintered silicon nitride (4,5,6,9).

- The specific heat vs. temperature of 2.2 gm/cc density reaction sintered Si_3N_4 was measured, as were thermal conductivity and thermal diffusivity vs. temperature for both 2.2 gm/cc and 2.7 gm/cc density reaction sintered Si_3N_4 (4).

- Stress-rupture data was obtained for reaction sintered silicon nitride under several conditions of load and temperature (6,9,10).

- A group of 31 2.7 gm/cc density injection molded Si_3N_4 test bars, made using the best current nitriding cycle and an atmosphere of 4% H_2, 96% N_2, resulted in a Weibull characteristic strength of 44.3 ksi and an m value of 6.8. Additional material development work is aimed at obtaining a higher m value (9).

- The effects of surface finish and post machining heat treatment on the room temperature strength of hot pressed silicon nitride were determined (10).

- The variation in MOR strength of hot pressed silicon nitride was determined from rotor-to-rotor, within one rotor, and as a function of initial material preparation (10).

- Room and elevated temperature flexure strengths of injection molded reaction sintered silicon nitride of 2.7 g/cc density were determined (10).

- No time dependent failures were observed for 2.7 g/cc density injection molded reaction sintered silicon nitride during stress-rupture testing for up to 200 hours at stresses of 20-30 ksi and temperatures of 1900-2200°F (10).

- A simple, practical approach, based on the Wiederhorn-Evans (11) theory, was derived to predict the life of a ceramic under load. The only material measurements required are two sets of strength values at two stress rates. For a given material, this would comprise a statistical number of bend tests (preferably > 30) at each of two stress rates for each temperature. Stress-reliability-lifetime design diagrams can then be readily constructed. Comparison of predicted lifetimes using this method agrees reasonably well with limited published experimental stress rupture data (11).

- Weibull MOR strength parameters were measured for "Refel" reaction bonded SiC at room temperature and five elevated temperatures. In addition, room temperature Weibull strength parameters in tension were measured but, using probablistic methods, did not correlate with the MOR strength data within a 90% confidence band. Suspected parasitic stresses in the tensile test and/or differences in specimen surface quality are being investigated (11).

Materials Science

- A technique was developed and applied to perform quantitative x-ray diffraction analysis of the phases in silicon nitride (2).

- An etching technique was developed and used for the study of the microstructure of several types of reaction sintered silicon nitride (2).

- The relationship of some processing parameters upon the properties of reaction sintered Si_3N_4 were evaluated (3,4,5,6,10).

- The oxidation behavior of 2.2 gm/cc density Si_3N_4 was determined at several different temperatures. The effect of oxidation was found to be reduced when the density of reaction sintered Si_3N_4 increased (3,7).

- The relationship of impurities to strength and creep of reaction sintered silicon nitride was studied, and material was developed having considerably improved creep resistance (4,5,6,9).

- Fractography and slow crack growth studies were performed on reaction sintered SiC (5) and hot pressed Si_3N_4 (6,7).

- The development of sintered Sialon-type materials was initiated (7). The effects of yttria additives were being studied, especially in relation to the formation of glassy phases (8,10).

- A higher density (2.7 gm/cc) molded Si_3N_4 has been developed which will be used for component fabrication. Four point bend strengths of 43 ksi at room temperature were measured (8).

- An experimental study showed that high pressures did not facilitate nitriding of relatively dense silicon compacts. A parallel theoretical study showed that to store sufficient nitrogen within the pores and avoid diffusion, an impractically high pressure would be needed (8).

- Three techniques to improve the oxidation resistance of 2.7 gm/cc density injection molded Si_3N_4 were evaluated (9).

- Nitriding exotherms, resulting in localized silicon temperatures in excess of 1420°C, produced silicon "melt out" with resulting large porosity and lower strength. Eliminating these exotherms by controlling furnace temperature appears to be the key to uniform microstructure, fine porosity and higher strengths (10).

- Work on yttria-containing Sialons showed that melting occurred at about 1200°C whether or not the glassy phase was crystallized. A number of further experiments were conducted to prepare single phase sialons from either the $Si_3N_4/Al_2O_3/AlN$ or $Si_3N_4/Al_2O_3/AlN/SiO_2$ material systems. Further work on Sialons was terminated as a result of reductions in the overall program (11).

- Use of a programmed temperature/time nitriding cycle resulted in variations of the microstructure of reaction sintered Si_3N_4, depending on furnace load. To correct this, a control system was designed and built to control the furnace temperature/time cycle automatically to maintain a reasonably steady consumption of nitrogen (i.e. nitriding rate). Use of this automatic control was shown to produce 2.7 g/cc density Si_3N_4 with consistent, high quality microstructure over a wide range of furnace load (11).

- A fabrication technique for turbine components of reaction bonded SiC has been under development by molding a thermoset polymer filled with SiC particles, pyrolyzing the polymer to carbon, then reaction bonding the structure by the infiltration of molten silicon (11).

Non-Destructive Evaluation

- Ultrasonic C-scan techniques were developed and applied to the measurement of internal flaws in turbine ceramics (1,2,3,4).

- Sonic velocity measurements were utilized as a means of quality determination of hot pressed Si_3N_4 (2,3,5,9).

- A computer-aided-ultrasonic system was used to enhance the sensitivity of defect analysis in hot pressed Si_3N_4 (3,4,6).

- Acoustic emission was applied for the detection of crack propagation and the onset of catastrophic failure in ceramic materials (1,2,5,6).

- A method was developed and applied for the detection of small surface cracks in hot pressed Si_3N_4 combining laser scanning with acoustic emission (4).

- X-ray radiography was applied for the detection of internal defects in turbine ceramic components (2,3,4,5). Hidden flaws in as-molded stators and rotor blade rings were located by x-ray radiography (5,6,7). Such NDE of as-molded parts has been used to develop processes to make flaw-free components (8).

- A dye penetrant has been used to detect surface cracks in components made of the 2.55 gm/cc density Si_3N_4 (8).

- A state-of-the-art summary of NDE methods as applied to the ceramic turbine programs was compiled (6).

- 500 injection molded blade rings were examined, most of them in detail using 30X magnification and X-ray radiography NDE techniques (10).

- A blade bend test was applied to a number of rotor blade rings to assess their quality in terms of characteristic failure load and Weibull modulus. A distinct difference was demonstrated between blade rings nitrided in 100% N_2 and those nitrided in a 96% N_2/4% H_2 mixture, with the latter being approximately 30-40% stronger (11).

- Two test fixtures were designed, built and applied for the mechanical loading of stators either to failure or to a pre-determined proof load. One fixture simultaneously loads each stator vane, and the other pressure loads the stator outer shroud. Testing to a proof load, while not a direct method of detecting flaws, can be considered a form of NDE. From testing several stators in these fixtures, a marked improvement in failure load was shown for 2.7 g/cc density Si_3N_4 stators as compared to stators made from earlier 2.55 g/cc density material. In addition, low-load vane failures could be directly related to fillet cracks (11).

- A number of NDE techniques were reviewed for possible application to ceramic turbine components including Microfocus x-ray, infrared thermography, x-ray tomography, an electrostatic method, and holosonics (11).

2.3 FUTURE PLANS

Future plans for the next reporting period for the ARPA-supported portion of the program will be confined to testing of duo-density Si_3N_4 turbine rotors. Since 25 such rotors are now available for finish machining for hot spin and engine testing (See Section 3.1.2), continued fabrication of state-of-the-art rotors for testing has been stopped. Further fabrication process development is planned under the ERDA-sponsored portion of the program (See Volume 2 Future Plans). It is hoped that, if methods to improve the process are developed and if test results of state-of-the-art rotors are promising, a decision will be made to fabricate and test such improved duo-density Si_3N_4 rotors.

The plans under the remaining FY-77 funds of the ARPA program are twofold. First, modify the rotor attachment method to prevent shutdown failures caused by excessive temperatures and to verify this by an engine test; and second, to test six duo-densty Si_3N_4 turbine rotors at a fixed speed and temperature in the hot spin test rig with an objective durability on each of 25 hours. (25 hours of the 200-hour ARPA duty cycle is at maximum speed and temperature.) Latest estimates of rotor reliability based on material time-dependent characteristics will be used as a basis for selecting the speed and temperature conditions for the 25-hour hot spin test.

Once the above is completed, currently planned FY-78 funds will be used to attempt a 200-hour composite ARPA cycle test of a duo-density Si_3N_4 rotor in the hot spin rig. The maximum conditions selected will be based on latest analyses and reliability test results.

3.0 CERAMIC COMPONENT EVALUATION

3.1 DUO-DENSITY SILICON NITRIDE CERAMIC ROTORS

Summary

A number of rotor blade rings and duo-density rotors were fabricated during this reporting period, incorporating, wherever possible, process improvements developed under the ERDA supported Ceramic Turbine Technology Program.

Over 600 rotor blade rings were injection molded utilizing the automatic solid state control system. Yield of blade rings having no visible defects in the as molded state was over 70%. Controlling the boron nitride thickness during blade fill processing coupled with a modification of the hot press graphite tooling greatly improved the hot press bonding process. The yield of flaw free hot press bondings with these changes was 70%. This represents the most significant improvement in the yield of hot press bondings to date.

Finish machining of rotors continued as did non-destructive evaluation. Sub-surface flaws in blade rings, not detected in the as molded state, were found in most components after nitriding, machining and in some cases destructive inspection. Surface flaws that were not observed in the as molded state were also detected after nitriding. Blade bend testing was used to monitor the quality of blade ring nitridings to insure that only the higher quality nitrided blade rings were used to fabricate rotors for testing.

Eleven duo-density ceramic turbine rotors were cold spin tested to qualify them for further hot running. Ten of the eleven reached over 50,000 rpm without failing blades, with one rotor successfully qualified to over 70,000 rpm after failing one blade at 65,640 rpm.

Development of the hot spin rigs continued. A combustor flame out problem was solved choking both the combustor air and fuel supply. The durability problem of the rotor tip shroud/failure detector was resolved by the use of solid fused silica tip shroud. The rotor bolt material was changed from H-11 tool steel to Inconel 718 for higher temperature/time capability. In further development of the hot spin rig, a number of ceramic and metal rotors were tested accumulating 26 hours and 68 hours of hot testing respectively.

An important engine test of a duo-density silicon nitride rotor was accomplished. Rotor 1195, with the associated stationary ceramic components (nose cone, stator and tip shrouds), was successfully operated at an average Turbine Inlet Temperature (T.I.T.) of 2200°F and 45,000 rpm for 10 hours without incident. This same rotor, with 27 full length aerodynamically functional blades, and stationary flow path was subsequently run for 25 hours at 2250°F average TIT plus 1-1/2 hours at over 2500°F average TIT all at 50,000 rpm. Despite a cautious shutdown, a catastrophic failure occurred during the shut down of the engine due to an overtemperatured metal component used to mount the ceramic rotor. The total hot time on the rotor was over 37 hours, all but a few minutes at a TIT of 2200°F or higher, at speeds of 45,000 to 50,000 rpm, including 1-1/2 hours at 50,000 rpm and over 2500°F TIT. This unprecedented test is the first time a ceramic rotor has been operated at these speed/temperature/time conditions.

3.1.1 DUO-DENSITY SILICON NITRIDE ROTOR FABRICATION

Introduction

The duo-density ceramic turbine rotor fabrication process is a multi-step forming procedure beginning with an injection molded silicon metal blade ring and ending with diamond grinding the hot pressed silicon nitride rotor hub to finished dimensions. Subsequent to the injection molding step, the blade rings are burned out, to remove the organic binders, and nitrided to convert the silicon to silicon nitride. The blade ring is then encased in a slip cast blade fill and nitrided. The silicon nitride blade fill supports the blades and rim during the subsequent hot pressing step. The hot pressing operation forms the hot pressed hub, from silicon nitride powder, and simultaneously bonds the hub to the reaction bonded silicon nitride blade ring. The final step is diamond grinding the finished contour of the rotor hub. Coupled with these operations is continued usage of non-destructive evaluation techniques to monitor part quality at each process stage.

During this reporting period fabrication of duo-density, turbine rotors continued in order to supply rotors for testing. Improved processing techniques, developed in the Ceramic Turbine Rotor Technology Program, supported by ERDA, were incorporated into the fabrication program wherever possible.

Injection Molded Blade Ring Fabrication

The last interim report[11] described the implementation of the automatic process control unit. During this current reporting period approximately 600 blade rings were molded utilizing this control unit to refine the molding parameters which resulted in an increase in the yield of usable green parts. Five hundred of the 600 blade rings were molded with an automated mold release system incorporated.

The improvements in both the processing of injection molded material and injection molding are covered in Volume 2 of this report which was supported by ERDA — Division of Transportation. The increase in yield of good as molded parts as a function of control development is shown in Figure 3.1. The bottom curve represents blade rings having no visible defects, in the as molded state, under 70X

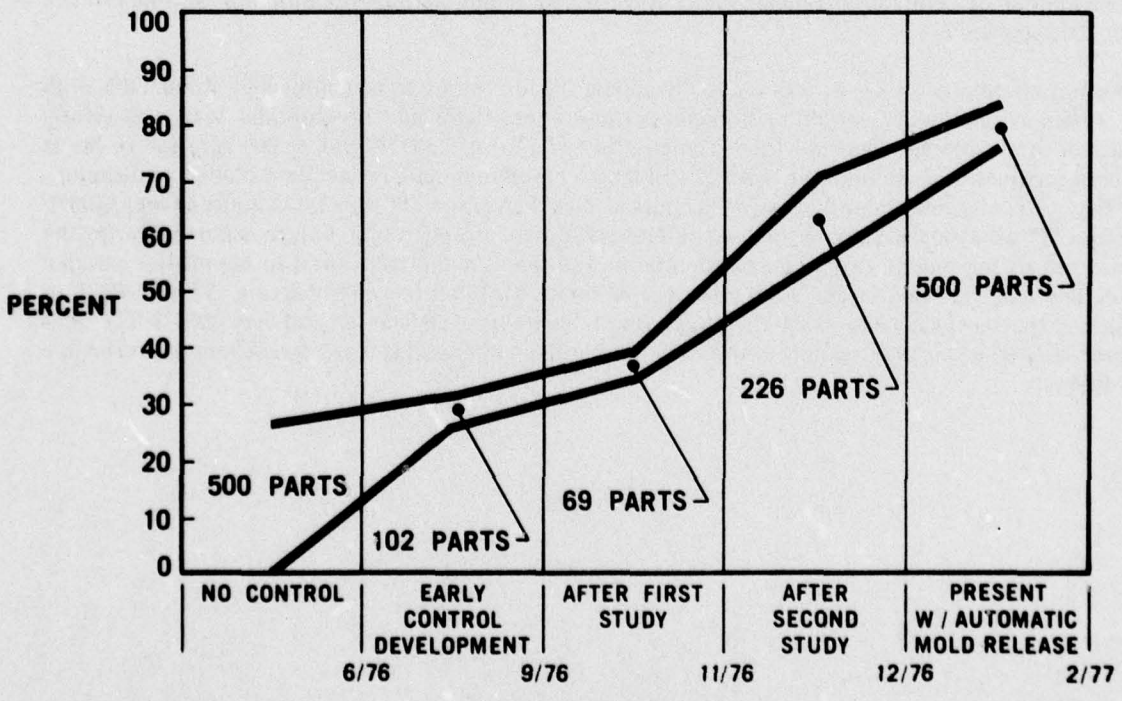

Figure 3.1 — Yield of Good As-Molded Blade Rings

microscopic inspection. The top curve represents usable test blade rings and includes those molded with no cracks or other functional defects and less than two minor surface imperfections. The number of parts refers to the total number of blade rings molded during a particular stage of control development. It should be noted that flaws were detected in some of these components after subsequent processing steps (see Volume 2 of this report). Improved NDE techniques being investigated may reveal more flaws in as molded components decreasing the yield of good parts.

Blade Fill Processing

After the blade ring had been fabricated and nitrided, the next step in the process was to slip-cast the blade fills which completely encapsulated the airfoils and the blade ring rim. The mechanical aspects of this process were described in a previous report[10]. The purpose of the blade fill is to provide support for the blades and the rim during the hot press bonding operation when the dense silicon nitride rotor hub is formed and bonded to the blade ring.

One modification which resulted in increasing the yield of hot press bonded rotors was developed under the ceramic processing technology effort funded by ERDA — Division of Transportation — in the Ceramic Turbine Rotor Technology Program. This change in the blade fill process, consisted of accurately controlling the boron nitride thickness which was used as a lubricant for subsequent blade fill removal and also served as a barrier material which prevented blade ring to blade fill bonding during the nitriding step (see Volume 2 of this report).

The other changes to the blade fill process were limited to the types of slips employed. Refinements were made in slip formulation and preparation so that a higher degree of reproducibility was obtained from lot to lot. Silicon metal comminution was standardized at wet milling for seven hours with tertiary butyl alcohol in one gallon polyethylene jars with high purity, high density aluminum oxide grinding media at a speed of 90 rpm. Slips were formulated using alkaline deflocculants and maintained at a pH of approximately 7.3. Silicon nitride grog (5 w/o) was added to yield a final nitrided density of 2.55 to 2.65g/cc after nitriding.

Hot Press Bonding

The fabrication of duo-density turbine rotors continued to utilize the simplified two piece concept introduced in the last interim report[11]. This concept, shown in Figure 3.2, eliminated the complex shape of the hub, thereby making possible densification of the silicon nitride powder at pressures far below those previously required to produce a dense fully contoured hub. During the last reporting period ten trial runs were made to this configuration which all resulted in blade and/or rim cracking to some degree.

During this reporting period a standard set of hot pressing parameters was established. Over fifty hot press bondings were made at 1000 psi pressing pressure, 1000 lbs wedge load, 1715°C for three hours using wet WC milled silicon nitride powder with 3-1/2 w/o magnesium oxide densification additive.

One modification which resulted in a significant improvement in the process was developed under the ceramic processing technology effort funded by ERDA — Division of Transportation — in the Ceramic Turbine Rotor Technology Program. This was a graphite tooling change to achieve more consistent functioning of the graphite wedge system (see Volume 2 of this report).

Thirty-two out of 46 rotors hot pressed with controlled boron nitride thickness and the graphite tooling modification had no detectable flaws or damage due to hot pressing. This represents a 70% yield of flaw free hot pressings.

Eight rotors, pressed to the standard conditions, were selected for materials characterization. The hub areas of these rotors were subsequently cut up for test bars of the hot pressed silicon nitride. Twenty-five rotors were designated for engine and hot spin rig testing. Thirteen rotors were set aside for blade bend and cold spin testing.

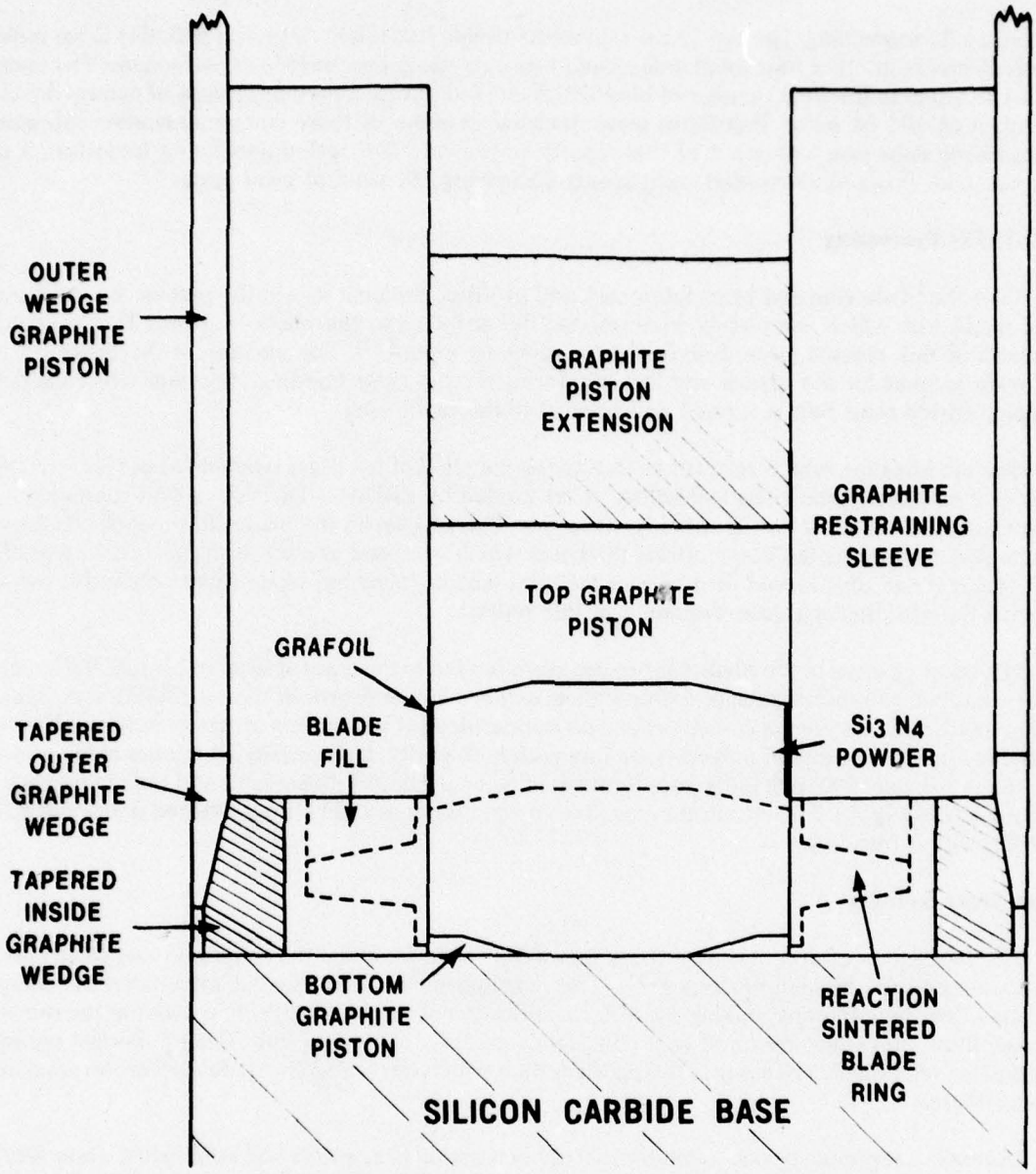

Figure 3.2 — Simplified Two-Piece Hot Press Bonding Configuration

Finish Machining

The first step in the process was to protect the rotor blades from machining and handling damage with a wax potting agent as shown in Figure 3.3. A Silastic™ mold was used to cover the blade tips *prior to the wax encapsulation* to prevent the build up of wax on the grinding wheel as the blade tips were machined. The leading edges of at least three of the blades were left exposed to establish the proper axial location of the datum surface.

The first grinding operation was to face off the rotor hub square in relation to the rotor blade gage surface. Having established this new gage surface, the rotor bore was rough core drilled from each side using a 7/16 inch diameter diamond plated core drill. An internal diamond grinding operation was then employed to finish the centerbore to the required one half inch diameter. All surfaces subsequently ground were finished concentric to or perpendicular to the centerbore.

A universal grinder, using the O.D. of a conventional diamond matrix wheel, was then used to rough grind the hot pressed hub surfaces. The disk contour was subsequently ground using a 140 grit diamond plated wheel (Figure 3.4) which was replated after finishing six rotors.

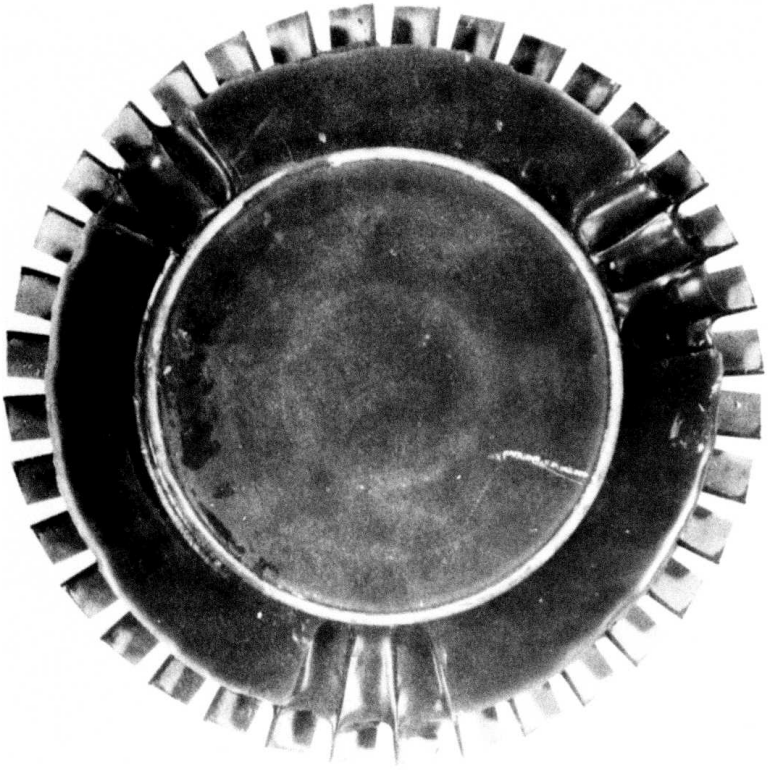

Figure 3.3 — Wax Potted Rotor Prior to Finish Machining

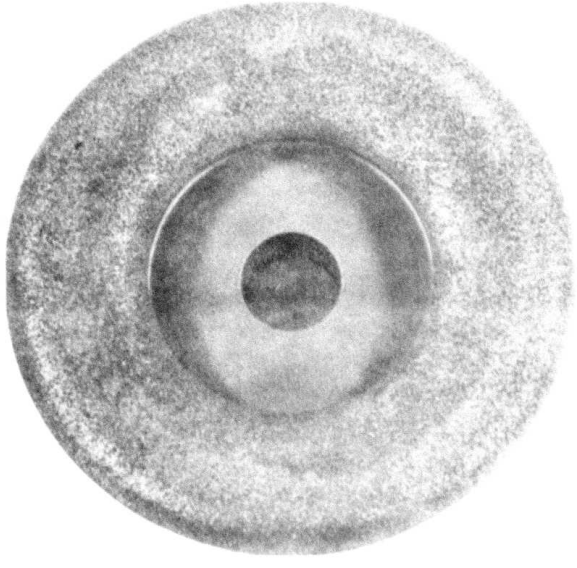

Figure 3.4 — Diamond Plated Rotor Contour Grinding Wheel

The counterbores, on the forward and aft surfaces of the rotor hub adjacent to the rotor bore, were ground using diamond plated form wheels on an I.D. grinder. The final grinding operations reduced the blade lengths to the requred O.D. and incorporated the required edge radii using a universal I.D./O.D. grinder. Figure 3.5 shows a finish machined rotor. The disk centerbore and throat areas were subsequently hand polished to achieve the specified 10μ surface finish.

Rotors which were scheduled for engine testing were further machined by grinding curvic coupling face splines on the forward and aft mounting surfaces.

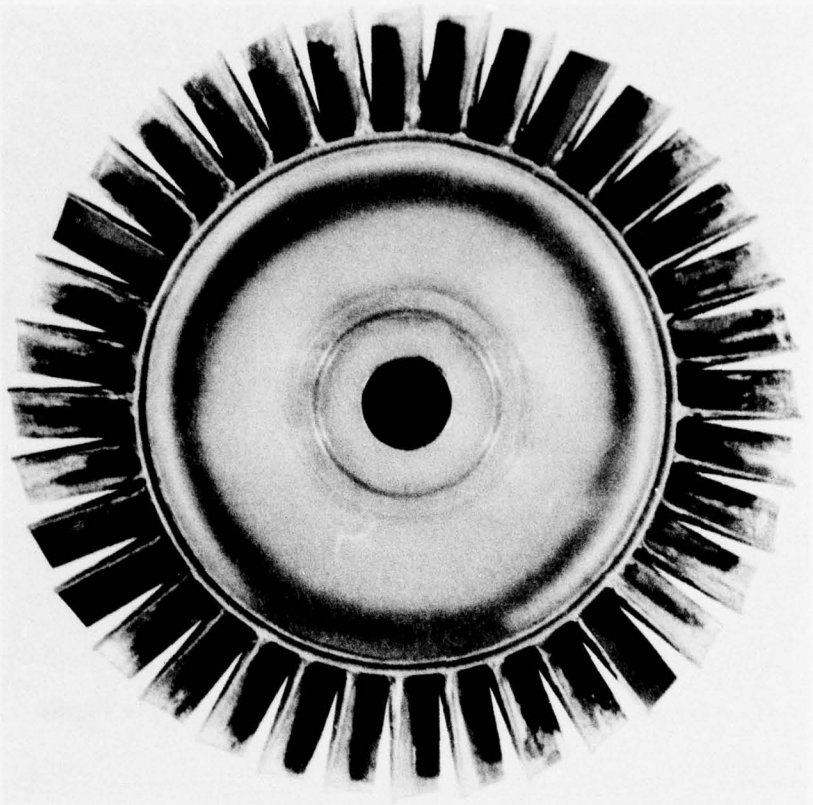

Figure 3.5 — Finish Machined Duo-Density Turbine Rotor

Non-Destructive Evaluation

Visual inspection, at 30-70X magnification, continued to be the most reliable technique employed for detecting surface flaws in rotor blade rings and stationary ceramic flow path components. A system of code letters was used to define the type of flaw observed and this information along with the location of the flaw was entered on an inspection form.

Table 3.1 shows the overall quality rating system established for nitrided rotor blade rings and finished duo-density turbine rotors. This system takes into account both the quantity and type of defects observed with a quality level of 1 having no detectable defect while a 5 indicated a poor quality component suitable only for experimental fabrication purposes or bench testing. The first rating a blade ring received, after nitriding, was considered preliminary because defects in the rim area were quite often removed during subsequent machining steps and in some cases new defects were revealed or introduced during the duo-density rotor fabrication process.

Three types of defects, which were the most difficult to detect, were: (1) defects in the rotor blade ring rim, (2) internal flaws in blades and (3) back and front side defects in blades that did not extend to either the leading or trailing edges of the blades.

TABLE 3.1

Blade Ring Quality Definition

Rating	Criteria
1.	No detectable defect.
2.	Blade ring can contain certain imperfections that would not result in a blade removal prior to testing. Examples of these imperfections are (1) Fold lines and small blade chips (2) Imperfections in rim no greater than 0.050 inches length with no visually detected depth.
3.	Same blade quality as Grade 2. Maximum of 8 rim flaws greater than 0.050 inches.
4.	Contains maximum of 8* flawed blades and rim imperfections greater than 0.050 inches.
5.	Contains axial rim cracks and/or flaws in blades and rim that would necessitate the removal of more than 8 blades.

* Total of 8 maximum, blade plus rim flaws.

Defects in the rotor blade ring rim were usually not characterized until after the injection molded center disk was removed and the I.D. of the nitrided blade ring was diamond ground. The majority of rim defects were believed to be the result of differential thermal contraction between the center disk and blade ring rim which occurred during the injection molding process. This type of defect (Figure 3.6) started in the center disk as a crack at an angle of 15 to 30 degrees to the rim. Most of the crack was removed during I.D. grinding resulting in a series of voids or low density areas at the terminus of the crack. This was usually the case when a crack in the center disk/rim fillet region was detected immediately after nitriding. However, in some cases, no crack was detected after nitriding but after I.D. grinding voids were revealed which were formed during molding, probably from entrapped gas.

Internal blade flaws (Figure 3.7) were not visually detected during processing but were observed in some blades which were cold spun or subjected to the blade bend test. This type of flaw would not necessarily be detected by the blade bend test as it could be located in a region of the blade cross section which was subjected to compression or a low tensile stress. In the future, microfocus X-ray techniques will be investigated to detect this type of defect.

The back side surface defect shown in Figure 3.8 was detected during visual inspection. However, because of the location of this type of flaw relative to the adjacent blades, the line of sight of the microscope and the direction of lighting is very important. Back side flaws grossly reduce the mechanical bend strength of the blades as they are located in a region of high tensile stress during bending.

Quality Monitoring

During previous reporting periods[9,10,11] blade bend testing was conducted on silicon nitride rotor blade rings primarily to develop the equipment and establish a repeatable procedure. A limited number of investigations were carried out on injection molded and slip cast blade rings[10] and on various nitriding atmospheres[11]. During this reporting period blade bend testing was used as a quality control tool to evaluate the nitriding of blade rings.

The data in Table 3.2 represents the test results from several nitridings made during this reporting period. The strength and Weibull modulus values of all these nitridings were acceptable except for the

B-83 nitriding. All parts in this nitriding were removed from the fabrication process because of the low strength values.

Blade bend test results were not used as the sole acceptance/rejection criteria because this type of test is not sensitive to the presence of unreacted silicon. Weibull strength and modulus values for B-80 and B-81 nitridings were acceptable, with the modulus values among the highest obtained, however, visual examination of the blade rings showed the presence of unreacted silicon. Since previous testing[9] indicated a reduction in strength would occur after thermal shocking and/or thermal soaking, the parts from these two nitridings were also removed from the rotor fabrication process.

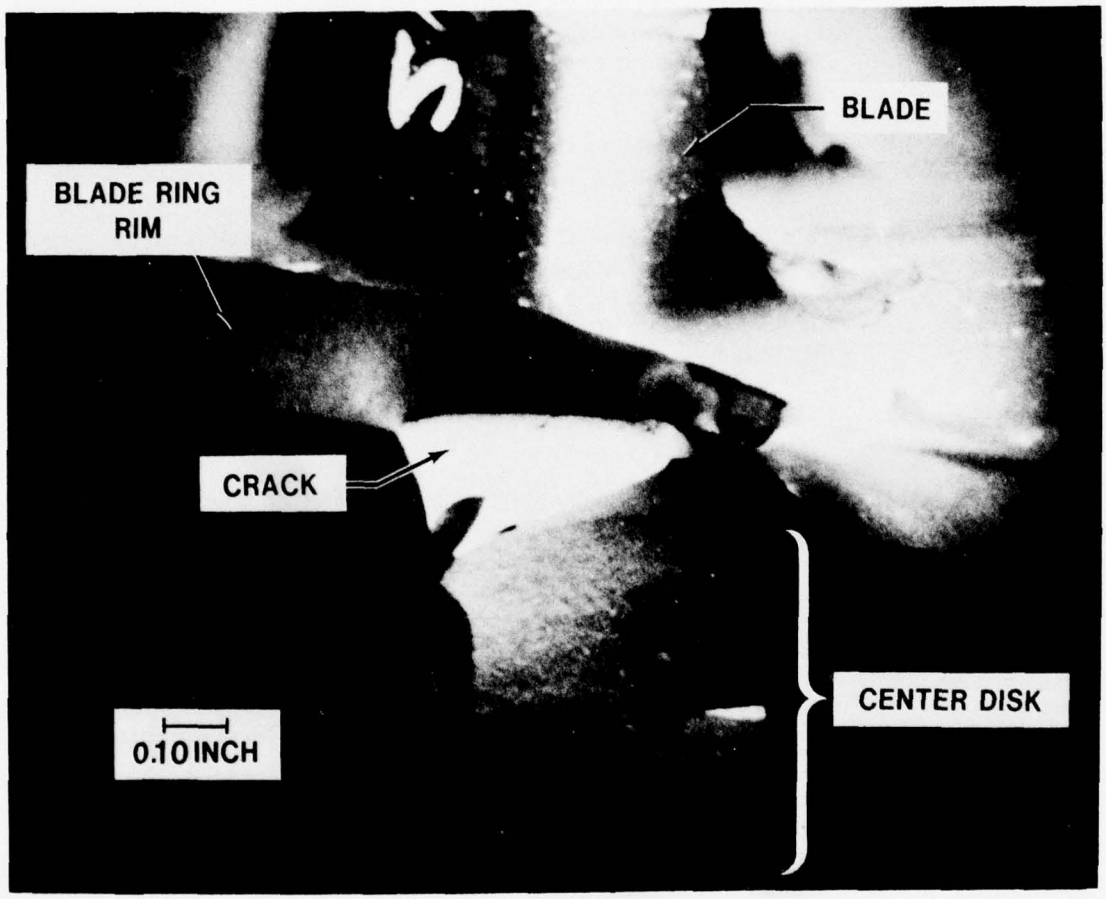

Figure 3.6 — Rotor Blade Ring with Rim Crack Defect

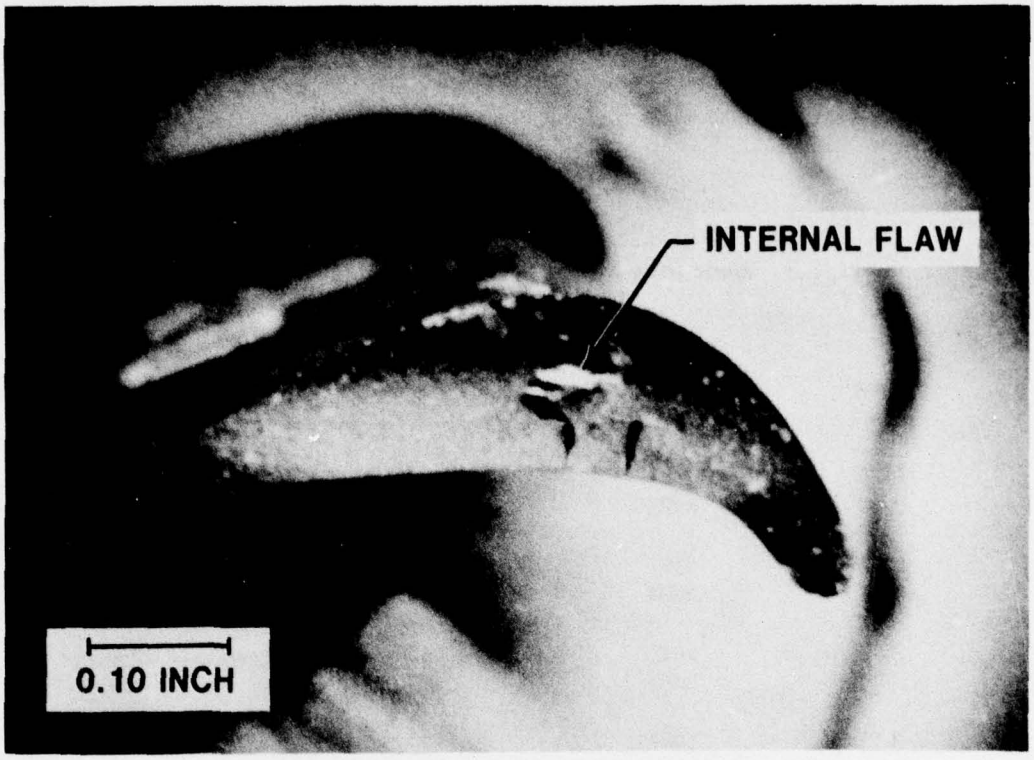

Figure 3.7 — Rotor Blade Internal Flaw

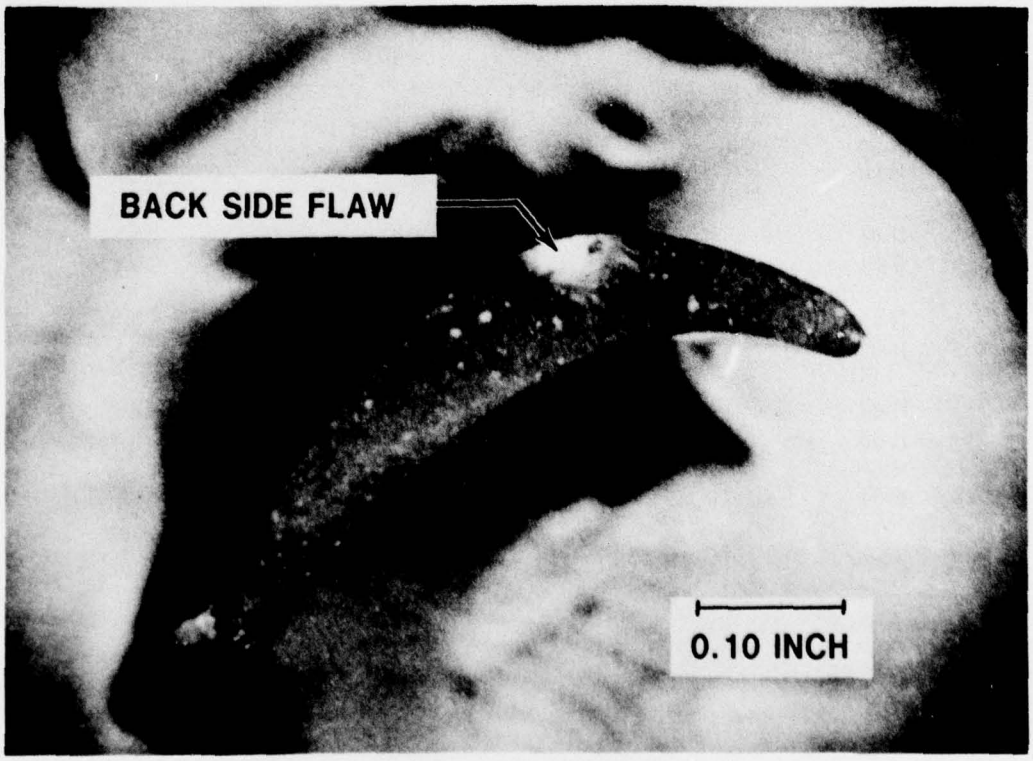

Figure 3.8 — Rotor Blade Backside Flaw

TABLE 3.2

Blade Ring Mechanical Load Testing Results

Brew No.	Blade Ring No.	Characteristic* Load (lbs.)	Weibull Slope
B-65	1980	87.9	7.5
B-65	1977	78.2	8.2
B-67	1991	85.4	11.5
B-67	2023	86.1	10.3
B-70	2047	85.5	11.4
B-70	2063	90.1	9.3
B-71	2064	83.7	12.6
B-71	2066	81.7	12.1
B-71	2067	79.4	10.7
B-78	2262	75.2	8.0
B-78	2280	81.2	9.2
B-79	2295	78.1	9.5
B-79	2302	81.1	17.0
B-80	2192	81.3	13.6
B-80	2318	74.9	16.8
B-81	2214	70.4	10.5
B-81	2325	80.5	14.1
B-82	2396	81.6	7.9
B-82	2455	70.8	9.8
B-83	2438	66.0	6.2
B-83	2575	59.6	5.5
B-84	2506	85.7	11.5

*Load at 63.2% failure rate.

3.1.2 DUO-DENSITY SILICON NITRIDE ROTOR TESTING

Introduction

During this reporting period the majority of rotors tested were fabricated utilizing the simplified two piece approach introduced in the last interim report[11]. Eleven duo-density silicon nitride rotors were qualified in the cold spin pit prior to hot testing. Hot testing continued primarily for the development of the hot spin test rig. Two of the seven hot rotor tests, one in the engine and one in a hot spin rig, represented major accomplishments during this reporting period.

Cold Spin Testing

The cold spin pit has previously been used to test rotor hubs, single blades and poor quality duo-density turbine rotors to failure[2,7,8,9,10,11]. During this reporting period twelve duo-density rotors were cold spun as part of a procedure to screen rotors prior to hot testing. The qualifying speed, selected for the cold spin test, was ten percent over the planned hot test speed to provide some margin for the additional thermal stresses imposed in hot testing. Any failure of the rotor blades prior to reaching the qualifying speed, required that the cold spin rig be shut down and the assembly re-balanced.

The test results are shown in Table 3.3. Rotor 1142 was fabricated using the three piece concept which was discontinued during the last reporting period because of inconsistent hot press to hot press bond joint strength. The remaining eleven rotors cold spun were fabricated utilizing the simplified two piece approach which eliminated this troublesome bond joint and no problems were experienced in the hot pressed material or in the hot pressed to reaction sintered bond joint. Five of the eleven rotors lost 1 or more blades at speeds ranging from 31,150 to 69,480 rpm. In each case at least one of the failed blades contained a flaw. Three of the remaining six rotors lost a small blade chip at the blade tip, one of these occurred at 63,620 rpm. Three of the rotors were qualified to 55,000 rpm without incident. It should be noted that three of the rotors which lost blades or a blade chip achieved over 63,000 rpm before failure.

Additional cold spin testing was conducted in the Turbine Rotor Technology Program which was supported by ERDA Division of Transportation. This work is covered in Volume 2 of this report.

Hot Spin Rig Development

Advancements made in ceramic materials and fabrication processes produced better quality rotors which resulted in longer test rig running times, higher speeds, and increased gas flow conditions. Consequently, test rig problem areas were identified which were not evident during earlier testing when rotors of poorer quality were utilized.

A combustor flame-out problem was encountered during rapid accelerations, when testing rotors with more than 25 blades. This was produced by a change in the pressure distribution around the naturally aspirated burners resulting in an adverse air/fuel (propane) mixture. The solution to this problem was to achieve choked flow conditions in both the combustor air and fuel supply thereby maintaining a constant air/fuel ratio regardless of the burner downstream pressure. The burners of the combustor were encased in a plenum which was supplied with air through a choked orifice (Figure 3.9). This plenum design also resulted in a more uniform velocity distribution to the individual burners. Also, an orifice was placed in the gas supply line to induce choked flow.

Attempts at high speed endurance testing, in the hot spin rig created a durability problem with the failure detection ring previously described[10,11]. The failure detector consisted of a thin ring of insulating material wound with closely spaced 0.010 inch platinum wire which provided a signal when broken by blade or rotor hub fragments. The increased operating temperatures for longer times weakened the sodium stabilized colloidal silica coating used to harden the surface of the detector insulation material. The action of the burned gases over the rotor blade tips then eroded the insulating material resulting in a failure of the detector ring.

TABLE 3.3

Cold Spin Test Results

Rotor Number	Speed RPM	Results
1142	20,200	Inner bond joint failure of 3 piece rotor
1195	45,380	Lost blade chip
	55,200	Rotor qualified
1211	55,000	Lost 4 blades at maximum speed, rotor qualified
1213	63,620	Lost blade chip
	65,000	Rotor qualified
1231	55,000	Rotor qualified
1256	31,150	Lost one blade
	55,130	Rotor qualified
1287	44,760	Lost blade chip
	55,000	Rotor qualified
1294	65,640	Lost 1-1/2 blades
	70,580	Rotor qualified
1296	55,040	Rotor qualified
1298	55,220	Rotor qualified
1309	52,720	Lost 1-1/2 blades
	55,030	Rotor qualified
1324	64,000	Lost 1 blade
	69,480	Lost 1 blade, damaged 3 adjacent, rotor qualified

The thickness of the insulation was increased from 0.125 to 0.750 inches even though this compromised the sensitivity of the detector to small blade segments. The coating material was changed to sodium free ammonium stabilized colloidal silica. Detectors of this configuration were fabricated and evaluated. However, the required initial life of 25 hours was not achieved. The durability problem was solved by changing the shroud from an insulating material to a solid fused silica ring. While the solid ring could not incorporate the platinum wire failure detector, it was successfully tested in a hot spin rig, with a metal rotor, for 25 hours. An out-of-balance detector on the rotor shaft is now used to detect rotor failures.

During previous reporting periods[9,10,11] the hot spin rig rotor bolt, made of H-11 tool steel material, was evaluated for short time tests and found to be satisfactory. During this reporting period five H-11 bolts were run for times from 31 minutes to nine hours to monitor creep elongation of the bolts (Table 3.4). Since permanent deformations were recorded, the temperature distribution of the bolt was determined by using temperature sensitive paints. Figure 3.10 shows the temperature distribution obtained when the bolt cooling air exit temperature was maintained at 410°F. Since the observed temperature near the threaded end of the bolt approached the temperature limit of the H-11 material (1000°F), the bolt material was changed to Inconel 718 which has higher temperature capability required for long time operation. Limited testing on one Inconel bolt, with ceramic rotors/hubs, indicated no creep after 3 hours.

During this reporting period, 26 hours and 22 minutes of hot testing duo-density silicon nitride turbine rotors was accumulated. An additional 68 hours and 24 minutes of hot testing was conducted with metal turbine rotors during combustor and burst detector/shroud development.

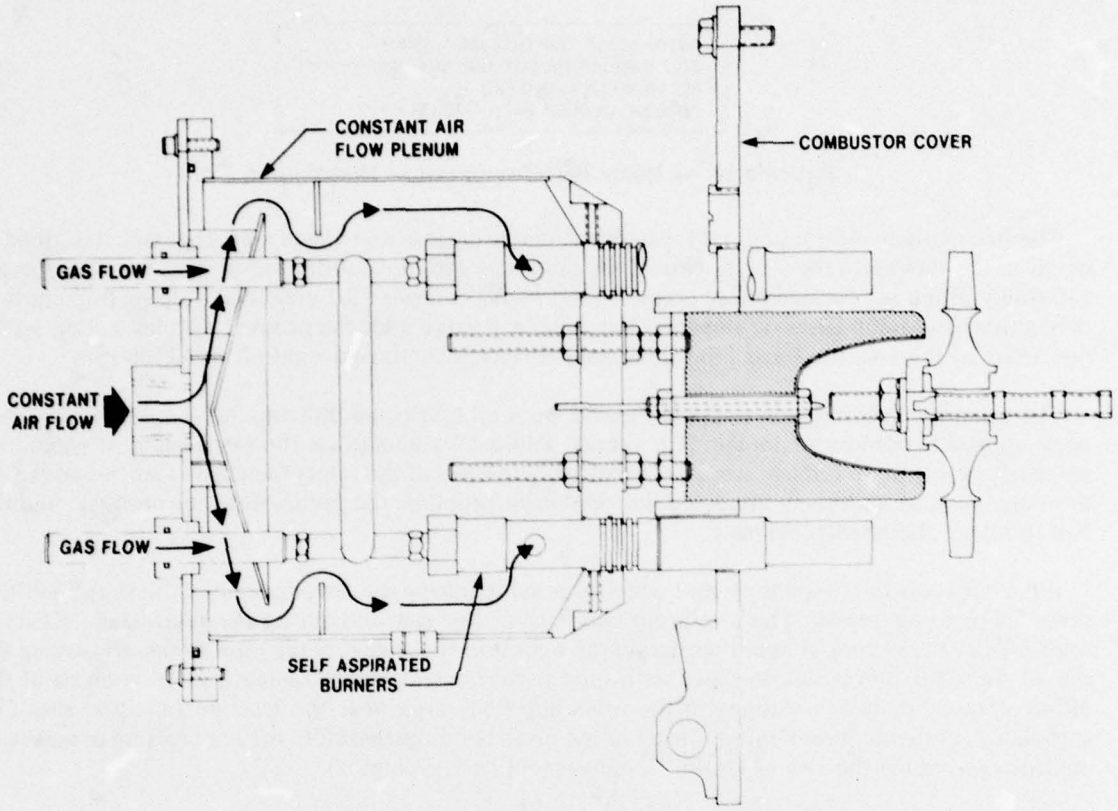

Figure 3.9 — Hot Spin Rig Combustor with Encased Plenum

TABLE 3.4

Creep Measurements H-11 Rotor Bolts

Bolt S.N.	Maximum Cooling Air Exit Temperature (°F)	Test Time (Hrs: Min.)	Maximum Speed (RPM)	Increase in Length (inches)
12	490	0:31	24,000	0.0006
17	310	0:40	24,000	0.0002
18	410	9:00	45,000	0.0014
20	350	0:49	50,000	0.0007
22	280	0:37	10,000	0.0009
22	360	2:20	50,000	0.0009

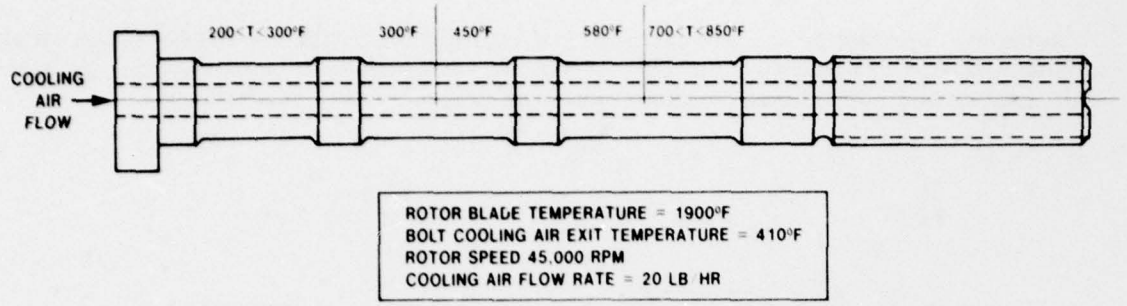

Figure 3.10 — Rotor Bolt Temperature Distribution

The first ceramic rotor tested, 1151, was fabricated using the three piece rotor approach described in detail in the 10th and 11th reports. One of the problems with this fabrication process was the strength variability of the hot pressed to hot pressed bond joint[11]. Rotor 1151 exhibited a strong zyglo indication at this bond joint, however since it was available, it was decided to proceed with hot testing. At the beginning of the test, the bond joint delaminated during combustor light-off at 10,000 rpm.

The remaining six ceramic rotors hot tested were all fabricated utilizing the simplified two piece rotor approach introduced in the 11th report. Table 3.5 summarizes the test results. It should be emphasized that these failures were not necessarily failures of the rotors themselves since parallel rig development was underway involving the combustor problem, the failure detector problem, and the bolt problem discussed previously.

Rotor 1184 was the first rotor tested which was made during the development of the simplified two piece hot pressing process. The combustor was fired at 2000 rpm and during a gradual acceleration the rotor failed at 3250 rpm. A small portion of the neck and rim region of the rotor broke off leaving the rest of the rotor hub bolted in place with nine partial height blades remaining. An analysis of the failure showed carbon inclusions in the rotor hub neck area near the fracture initiation site. The carbon was probably from Grafoil™ used in hot press bonding, therefore the hot pressing process was modified to reduce the risk of Grafoil™ entrapment (see Volume 2).

TABLE 3.5

Ceramic Rotor Test Results in Hot Spin Rigs

Test Date	Rotor Serial Number	Blade Ring Serial Number	Number of Blades During Hot Test	Speed (RPM) Cold Spin	Speed (RPM) Maximum Hot	Speed (RPM) At Failure	Rim Temperature Maximum	Rim Temperature At Failure	Total Hot Time (Hrs:Min)
2-12-77	1184	1816	24-1/2	—	3250	3250	1000	1000	0:03
2-16-77	1205	1985	21-1/2	—	53,000	53,000	2050	1985	0:37
6-1-77	1211	2034	24	55,000 (1)	2000	Δ	1900	Δ	0:20
6-20-77	1213	2008	26	65,000	43,000	43,000	1800	1800	4:50
4-14-77	1231	2003	17	55,000	30,000	Δ	1850	Δ	0:31
9-17-77	1256	2017	27-1/2	55,000 (2)	50,000	50,000	1840	1800	20:01

(1) Four blades failed at 55,000 rpm
(2) One blade failed at 31,150 rpm
Δ Failure detector not activated

Rotor 1205 sustained the initial light-off but excessive vibration was noted at 40,000 rpm and the rig was shut down. The rotor was inspected and a second run was initiated. An attempt was made to accelerate through the vibration speed range but a catastrophic failure occurred at 53,000 rpm and 1985°F rim temperature. Severe vibrations were also encountered during this second test.

Rotor 1211 was subjected to an experimental process, during fabrication, to remove the first blade fill. During cold spin proof testing, prior to hot testing, four blades were lost at 55,000 rpm. During the hot spin test, 17 minutes after light-off, a drop in the rotor rim temperature was noted, and the test was terminated two and one half minutes later. It appeared that four blades had spalled off at the rim at a low speed since they did not penetrate and activate the failure detector. The failure was attributed to weakened blade material due to the experimental fabrication process used (subsequently discontinued) to remove the first blade fill.

Rotor 1213, previously cold spun to 65,000 rpm without failure, was subjected to 10 light-off cycles in the hot spin rig where the rim temperature was cycled from room temperature to 1800°F without incident to investigate the effect of light-off as a cause of blade spalling. During the final run, a vibration increase was noted during a rapid acceleration from 30,000 rpm at 1800°F rim temperature. Failure occurred at 43,200 rpm, which activated the failure detector and an automatic shutdown followed. Fourteen blades were broken, all above mid-height, and the remaining blade tip leading edges showed signs of rubbing. Nearly all blade failures initiated at the leading edge side. In addition the turbine bearing had failed.

Rotor 1231 was cold spun to 55,000 rpm without incident. A combustor flame-out occurred at 24,000 rpm on the initial acceleration. The combustor was re-lit at 2000 rpm and the rotor accelerated to 30,000 rpm. After five minutes at this condition the test was terminated. Tear down of the rig revealed that all the blades were lost with several blades lying intact, in the exhaust duct and the failure detector was not penetrated indicating low speed failure.

Rotor 1256 lost one blade at 31,150 rpm during cold spin qualification but subsequently achieved 55,000 rpm without further incident. Two hot runs were terminated after encountering vibration problems and labyrinth seal rubs at 28,800 and 40,000 rpm. These problems were corrected by installing a new main shaft assembly and rotor 1256 was run for 18 hours and 42 minutes at 50,000 rpm and 1800°F rim temperature. The torque was seen to increase just before a catastrophic failure occurred.

As seen from the above, several of the tests conducted during this reporting period encountered excessive rotor shaft vibrations. A re-evaluation of the rotor mounting system was initiated to investigate the cause of the vibration. A ceramic hub was balanced with a conical adaptor and tested successfully in hot spin rig #2 to 50,000 rpm at ambient temperature. The rig was then operated at 2000 rpm and the rim temperature of the hub increased to 1800°F. Attempts to accelerate to 50,000 rpm resulted in high vibration and rotor shaft instability at approximately 35,000 rpm. The conical mounting system was then replaced with the more expensive curvic mounting system designed for the engine. A similar test was conducted with a ceramic hub mounted with the curvic couplings and was completely successful as no vibration was encountered, hot or cold. It was then decided that future hot spin rig tests would utilize the curvic coupling mounting configuration.

Rotor Failure Analysis

Introduction

Section 1.0 of this report described the iterative approach utilized in the Ford/DARPA ceramic development program. This comprehensive iterative development program involves the interaction of design, materials development, ceramic processes, component rig testing, engine testing, non-destructive evaluation and failure analysis. This section describes the failure analysis system and highlights some pertinent results from a typical failure analysis conducted after a hot spin test.

The purpose of failure analysis at this stage of the program is two-fold:

1. to determine the cause of failure in order to improve design, materials, fabrication and testing

2. to validate or invalidate rotor reliability test results by determining whether a given rotor failure was due to material inadequacy or extraneous causes such as improper testing or rig failure.

Procedure

The failure analysis procedure which has been employed for over a year involves a team approach. Inputs of data and opinions from scientists, engineers and technicians in various disciplines are gathered and a brief summary report is issued which usually includes recommendations for further action.

Chronologically, the failure analysis task starts with gathering information from the material development and component fabrication scientists and engineers. This includes chemistry, process and inspection reports. Any prior history, such as proof testing or prior service is also noted.

Next, the test objective, test equipment, and test schedule are obtained from the test engineer. After the test, data charts are reviewed with the test engineer. Another test engineer, not associated with this particular test, also reviews the results and sometimes watches the actual test to provide an independent opinion on the proper conduct of the test.

A stress analyst is also a member of the failure analysis team. He handles any stress or heat transfer calculations which may be necessary. In addition, materials engineers and design engineers analyze the fractures for clues to the cause of failure and to determine if the design was adequate.

The information gathered is summarized by the failure analysis coordinator and reviewed by all members of the team prior to distribution of the results to all key department personnel. While not one of the best rotors tested, an example, showing the highlights of the failure analysis on rotor 1231, follows:

Test Objective: The purpose of this hot spin test was to determine the long term reliability of rotor 1231, a duo-density silicon nitride turbine rotor.

Test Equipment: Hot spin rig number 1, build number 15 using main rotor shaft assembly number 3.

Test Schedule: The following steps were planned for this test:

1. Rotate rotor to 2000 rpm.
2. Light burners and accelerate to 10,000 rpm.
3. Adjust gas flow to increase the rotor rim temperature to 1700°F.
4. Maintain 1700°F rim temperature during gradual acceleration to 24,000 rpm.
5. Accelerate quickly to 41,000 rpm (in approximately 3 seconds) to avoid resonant vibrations previously encountered between these two speeds.
6. Accelerate gradually to 45,000 rpm monitoring rotor shaft clearance probe for any evidence of instability.
7. Readjust rim temperature to 1780°F at 45,000 rpm.
8. Operate at this steady state condition for 10 hours.
9. Decelerate to 2000 rpm in approximately 5 seconds.
10. Shut off burners and stop dynamometer while continuing to flow all cooling air.

11. Repeat cycle, steps 1-10, each following day but increase the rotor rim temperature by 50°F each day until 2030°F is reached.

12. Run the rotor at 2030°F and 45,000 rpm until failure occurs.

Data on Rotor 1231:

1. Rotor Design — Design D prime airfoil configuration with narrow throat disk contour — simplified two-piece construction.

2. Rotor Materials — The blade ring, serial number 2003, was injection molded reaction bonded silicon nitride of 2.7g/cc final density. The rotor hub was hot pressed from A.M.E. CP-85 silicon nitride powder with 3.5 w/o magnesium oxide added. Powder milling was batch number IH using tungsten carbide balls, methanol medium for 72 hours.

3. Fabrication Process — Blade ring 2003 was made by injection molding silicon powder and nitrided in nitridation run 67 utilizing the demand cycle with 96% nitrogen and 4% hydrogen. Simultaneous hot pressing of the rotor hub and bonding to the blade ring was accomplished utilizing the simplified two-piece approach at 1000 psi densifying pressure, 1000 pounds wedge restraining load, three hours at 1715°C, 0.040 inch tooling overhang and standard slip cast silicon nitride blade fill of 2.2 to 2.6g/cc density.

4. Machined Configuration — The rotor was machined to RTR-1505 (narrow throat). Blade stubs were ground to within 0.010 inches of the rim after the removal of defective blades.

5. Inspection — The blade ring was inspected in the molded state, after burnout, nitriding, initial machining, blade fill machining, press bonding and final machining. After initial machining 9 voids were noted on the inside diameter of the rim and two blades were cracked. After blade fill machining, 5 voids remained under blades 17, 18, 26, 27 and 28. Prior to cold spin testing 12 defective blades were removed. After cold spin testing an additional 7 blades were removed to balance the rotor leaving 17 blades to be hot spin tested.

6. Proof Test and Service History — Rotor 1231 with 24 full length blades was spun in a vacuum, at room temperature, to 55,000 rpm without incident.

Actual Hot Spin Test Conditions: On April 14, 1977, rotor 1231 was rotating at 2000 rpm when the burners were ignited. After accelerating to 10,000 rpm the conditions were held for three minutes to stabilize the temperature and then the rotor was accelerated to 24,000 rpm. The burners flamed-out after 30 seconds at 24,000 rpm. The speed was reduced to 2000 rpm and the burners re-lit. The rotor was accelerated to and stabilized at 10,000, 24,000 and 30,000 rpm. After five minutes, at 30,000 rpm, visual inspection indicated the blades were missing and the test was terminated.

Fractography: All blades were lost but the rotor hub was intact. Eight blades spalled off of the rim in three areas, and five of those were found lying in the exhaust duct. The eight spalled off blades were 10, 11, 12, 13, 27, 28, 34 and 35. Dimples in the rim fracture sites appeared to be defects in the blade rim. Several holes in the insulation around the rotor were made by blade fragments, but the failure detector wire was not broken.

Test Data Evaluation: The Visicorder chart showed the rim and turbine exit temperatures to be dropping slowly for 5 seconds, possibly due to flame instability, followed by a sudden, rapid drop due to flame-out. No datum was available to indicate when the blades broke off since the blade fragments which hit the failure detector ring did not rupture the failure detector wire to trigger automatic shutdown. The low impact energy of the blades indicated that the blades broke off at less than 24,000 rpm.

Summary: Failure speed and temperature are unknown, but the speed was much below 24,000 rpm. The spalling type of failure is attributed to diagonal shear induced by compressive stresses in the rim. These stresses could have resulted from residual stresses and abnormal thermal conditions in the test.

Void defects in the rim and the flame-outs and relights might have contributed significantly to the low speed failure of this rotor. Were this test made for rotor reliability distribution information, it would have been invalidated since failure could have been induced by burner flame-out and relighting.

Rotor Testing in the Modified Engine

The modified engine configuration was developed[10] so that a single axial turbine rotor could be tested in the engine at higher temperatures at a lower speed than planned for the two stage axial turbine. The modification reduced the regenerator inlet temperature to an acceptable level by using combustor inlet and compressor discharge air to dilute the hot gases exiting from the single stage turbine before entering the regenerator. This configuration was utilized to test rotor 709 which had ten blades of 90% length[10]. Subsequent analysis of the test data and inspection of the regenerator cores indicated that the amount of bypass air could be reduced on future runs without overtemperaturing the regenerator cores.

Since the duo-density ceramic turbine rotor to be tested during this reporting period contained more blades of longer length and therefore would extract more work from the hot gases and further reduce the turbine exit temperature from that experienced in 709's run, only the compressor discharge bypass route was employed (see Figure 3.11). This configuration was a step closer to the original design engine as more air was routed through the turbine flow path.

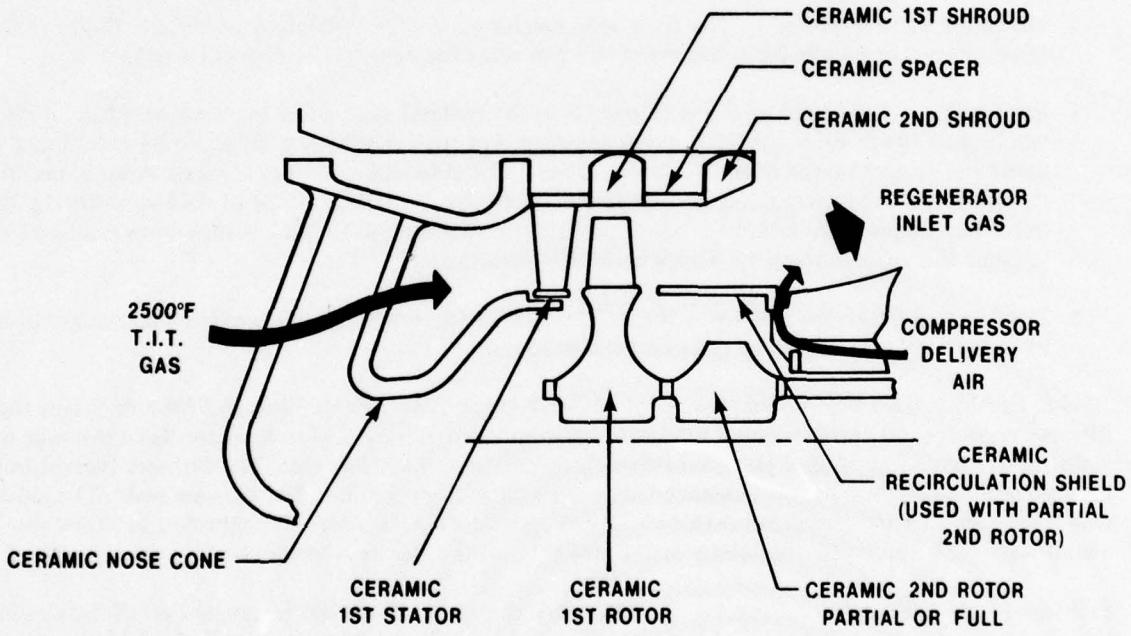

Figure 3.11 — Cross Section of Modified Engine Flowpath

Rotor 1195 Description

Rotor 1195 was the second, fully machined, design D prime duo-density ceramic turbine rotor produced using the simplified two-piece fabrication concept described in detail in reference 11. The 2.7g/cc reaction sintered silicon nitride blade ring (produced by injection molding) was hot press bonded to the hub while simultaneously hot pressing the hub from silicon nitride powder containing 3.5 w/o magnesium oxide densification additive. The assembly was then diamond ground to final dimensions using the procedure outlined earlier in this report. Figure 3.12 shows the finished rotor and attachment hardware prior to testing.

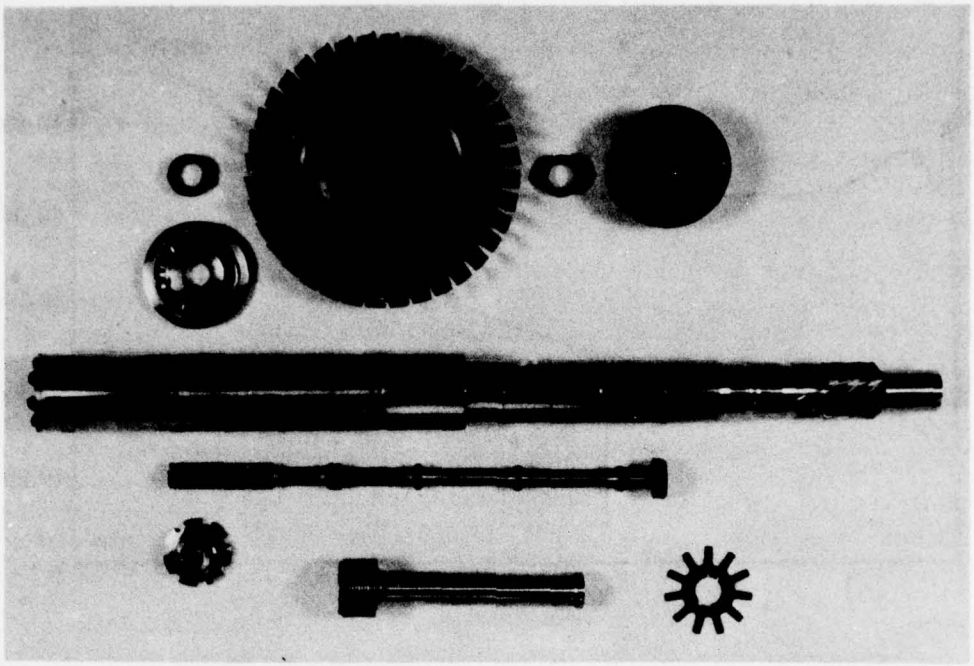

Figure 3.12 — Ceramic Turbine Rotor 1195, Attachment Hardware and Main Shaft

Since this rotor was produced while developing the duo-density rotor fabrication process several defective blades were removed to reduce the risk of failure during cold spinning and hot engine testing. A total of eight blades were removed; five because of voids in the rim under the blades, one which was cracked during injection molding, one which was cracked during hot press bonding and one to reduce the unbalance. In addition, one half of one of the remaining 28 blades was broken off during handling. The blade tip diameter was reduced from the blueprint dimension of 4.631" to 4.542" to provide an additional 0.045" radial tip clearance to reduce the risk of tip rubs. Prior to the engine build the rotor was spun to 55,200 rpm in the cold spin pit as described earlier in this report.

Test Results

The initial test of ten hours of steady state operation at 45,000 rpm and 2200°F turbine inlet temperature was accomplished with complete success. The start up and shutdown portions of the test are shown in Figures 3.13 and 3.14. The post run inspection of the rotor (Figure 3.15) and associated ceramic flow path hardware showed the parts to be in excellent condition. Dimensional checks of the rotor and mounting bolt indicated no permanent deformations had occurred. The gold plated curvic teeth on the metal adaptor and the main rotor shaft were in very good condition and appeared identical to developmental test results described in the last report[11].

The same parts were then reinstalled for further testing at higher speeds and temperatures. The start-up, Figure 3.16, was very similar to the first test and after conditions stabilized the engine was run for 25 hours at 2250°F average turbine inlet temperature and 50,000 rpm without incident. The average turbine inlet temperature was then increased to 2530°F (2477 to 2582°F) for an additional one and one-half hours at 50,000 rpm.

During the course of the last phase of this 26-1/2 hour run it was observed that the measured gas temperature in the rotor front face cavity, shown in Figure 3.17, had approached 1900°F. This was cause for concern since it was considerably in excess of design expectations (i.e. 1150°F). Prior furnace testing of the metal curvic adaptor to ceramic curvic rotor interface indicated potential damage due to interface friction at high temperature. A gradual shutdown was started by decreasing turbine inlet temperature while maintaining 50,000 rpm, but catastrophic failure occurred six minutes into the shutdown with the turbine inlet temperature at 1900°F.

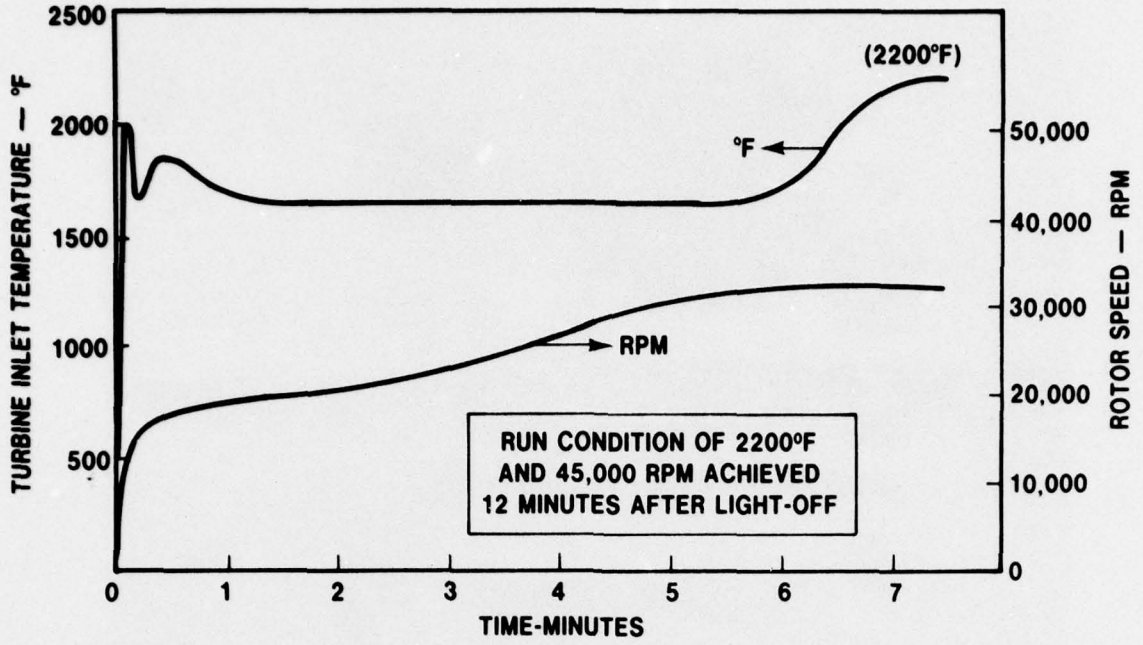

Figure 3.13 — Start Transients of Initial 10-Hour Run of Rotor 1195

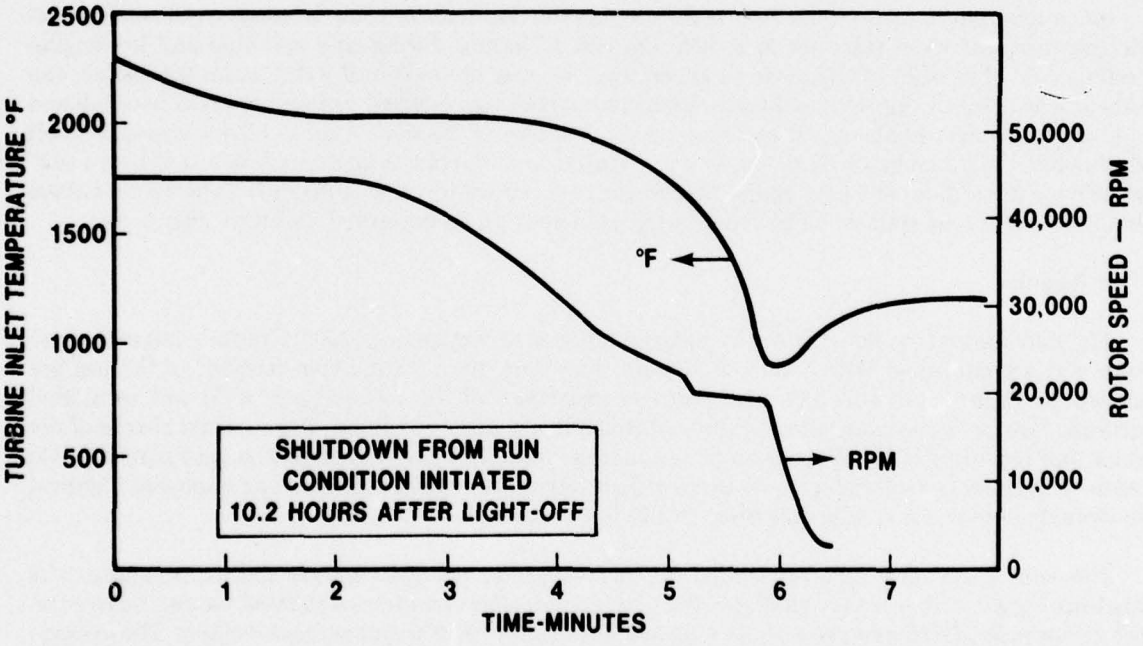

Figure 3.14 — Shutdown Transients of Initial 10-Hour Run of Rotor 1195

The failure was completely contained within the inner portion of the engine main housing but caused extensive damage to the ceramic components. In order to determine the cause of the failure, reconstruction of the components was attempted. Figure 3.18 shows a front view of the reconstructed nose cone. It was noted that most of the smaller and missing pieces were located in the plane of the rotor hub. Examination of these fracture surfaces indicated a mechanical type of failure occurred emanating from the inside of the bell lip and probably caused by pieces of the rotor striking the lip of the nose cone.

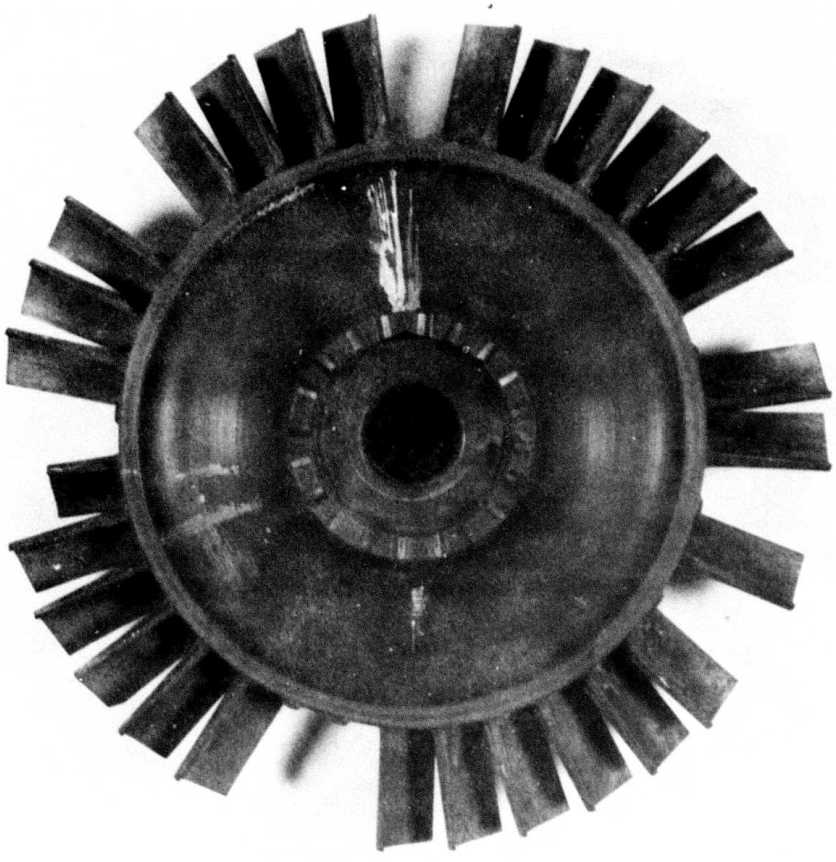

Figure 3.15 — Rotor 1195 after 10-Hour Run

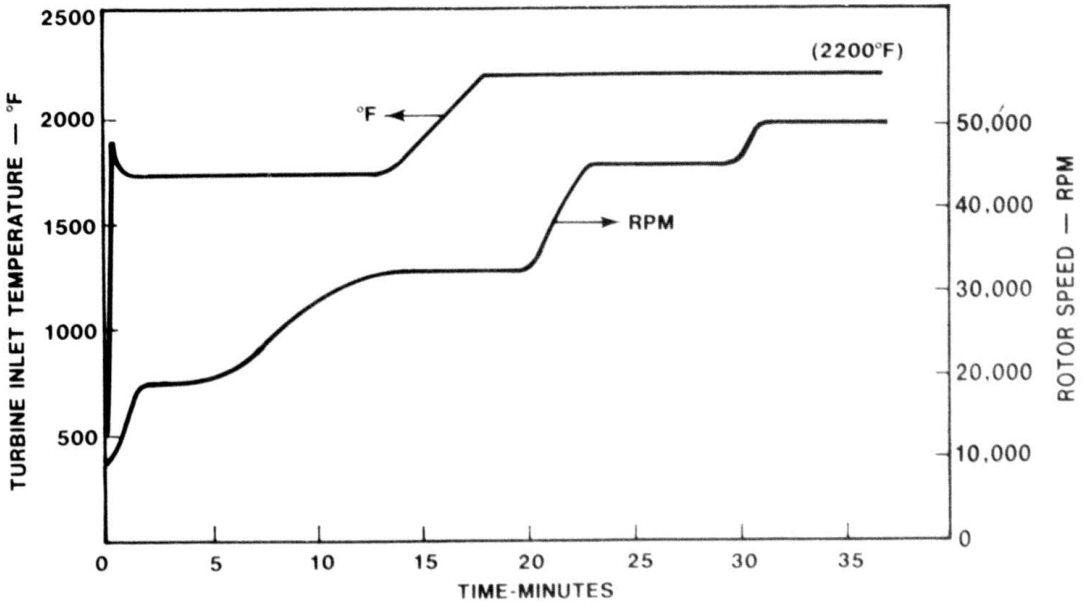

Figure 3.16 — Start Transients of 25-Hour Run of Rotor 1195

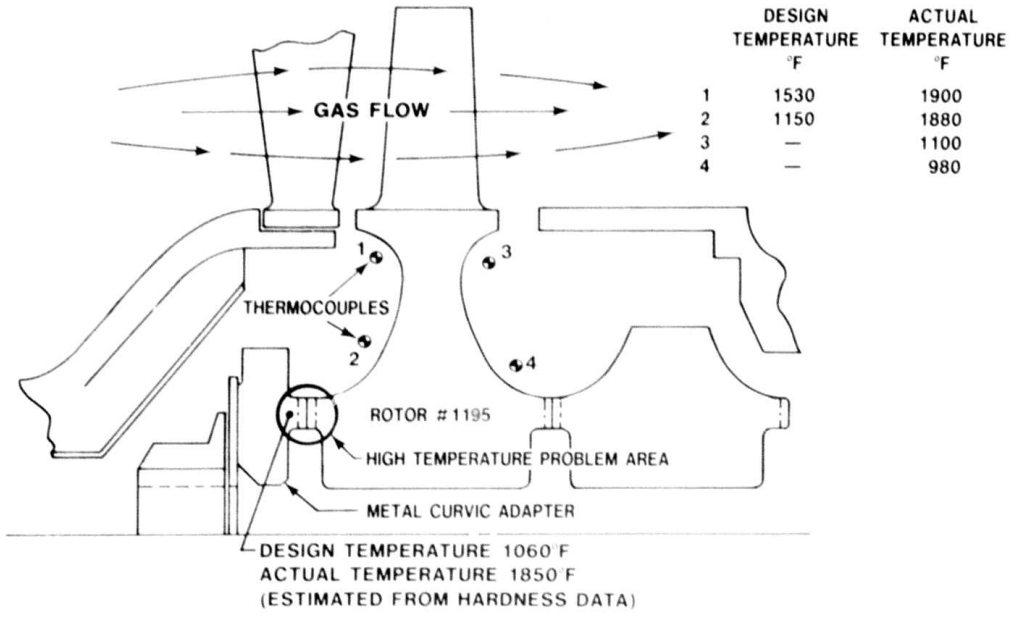

	DESIGN TEMPERATURE °F	ACTUAL TEMPERATURE °F
1	1530	1900
2	1150	1880
3	—	1100
4	—	980

Figure 3.17 — Cross-Sectional View Showing Rotor Front Face Cavity

Figure 3.18 — Reconstructed Nose Cone after Failure of Rotor 1195

Figure 3.19 shows a front view of the reconstructed Rotor 1195. Close examination of the ceramic curvic mounting teeth indicated that they had been sheared off by a radially inward force. Examination of the mating metal curvic adaptor showed that the adaptor had been severely overheated causing the curvic teeth to soften and resulting in pieces of the ceramic curvic teeth being embedded in and stuck to the surfaces of the metal adaptor teeth. Hardness checks on the metal curvic adaptor near the curvic teeth indicated the metal had reached 18-1850°F (compared to a design temperature of 1060°F).

Figure 3.19 — Rotor 1195 Reconstructed after Failure

From this data, it was concluded that the cause of failure was the overheated metal curvic adaptor which had seized to the ceramic rotor curvic teeth, and then broke off these teeth as it cooled down during the engine shutdown procedure. In view of these findings the metal to ceramic interface cooling will be modified before the next rotor test.

At the time of failure, rotor 1195 had operated in the modified engine for 37 hours and 19 minutes. All but a few minutes of this running time was on uncooled ceramic components at unprecedented turbine inlet temperatures of 2200°F or higher and at 45,000 to 50,000 rpm. This included one hour and thirty minutes of operation at 2500°F and 50,000 rpm.

3.2 CERAMIC STATOR, SHROUD, NOSE CONE AND COMBUSTOR DEVELOPMENT

Summary

Fabrication development on injection molding of stators and nose cones of 2.7g/cc density was continued on a limited basis. Following some alterations in the tooling a group of stators were molded, processed and mechanically tested at a loading of 20 pounds per vane. Some additional reaction sintered silicon carbide stators were also fabricated because of promising test results previously presented[11]. Nose cones were injection molded after the tooling was improved to prevent premature movement during core pin withdrawal, resulting in apparent elimination of a previous cracking problem at the strut fillets[11]. As a back-up approach, a method of fabricating reaction bonded silicon nitride nose cones by slip casting was investigated, and a nose cone was successfully produced for testing.

Testing of stationary components continued in both qualification and durability rigs. Stators were subjected to more severe qualification tests as the vane bend load was increased from 10 to 19 pounds and the outer shroud pressure load was increased from 100 to 200 psi. Both of these changes were made to eliminate weak or flawed components prior to engine or rig testing. Weight gains of components were monitored during hot testing at 1930 and 2500°F and found to be below previously observed values for several injection molded parts. Over 1000 hours of hot testing was accumulated on stators during this reporting period.

A complete set of silicon nitride stationary components consisting of a nose cone, two stators, two rotor tip shrouds and a second stage stator centering ring completed the program objective of 175 hours at 1930°F plus 25 hours at 2500°F with over 40 lights. In addition a silicon carbide stator successfully completed over 175 hours at 1930°F plus over 28 hours at 2500°F with 52 lights.

Thus stators of two different materials, injection molded reaction bonded silicon nitride and reaction bonded silicon carbide, have now completed the program durability goal of 200 hours.

3.2.1 FABRICATION

Introduction

The primary emphasis of the Ceramic Turbine Testing program, during this reporting period, was on the fabrication and testing of duo-density ceramic turbine rotors. However, engine testing of ceramic rotors requires the use of stationary ceramic components and therefore a moderate effort was expended on fabricating silicon nitride nose cones and stators. During the last reporting period, the fabrication of 2.7g/cc injection molded silicon nitride stators and nose cones was initiated but cracking problems in the green "as molded" state, were encountered in both components[11]. These problems were addressed during this reporting period

Silicon Nitride Stators

Fabrication of injection molded reaction bonded silicon nitride stators at the 2.7 g/cc density level was continued during this reporting period. As previously reported[11], a cracking problem had been experienced at the I.D. shroud due to sticking of the part in the sprue entrance detail of the tool. To eliminate the sticking, the sprue detail was teflon coated and several stators were molded. The sticking at the entrance (see location A in Figure 3.20) was eliminated. However, one area at the material overflow (see location B in Figure 3.20) continued to stick. It was determined that this sticking was due to overheating of a local spot in the die. The overheating resulted from restricting the material flow in the gate and by closing the overflow reservoir, the overheating was eliminated.

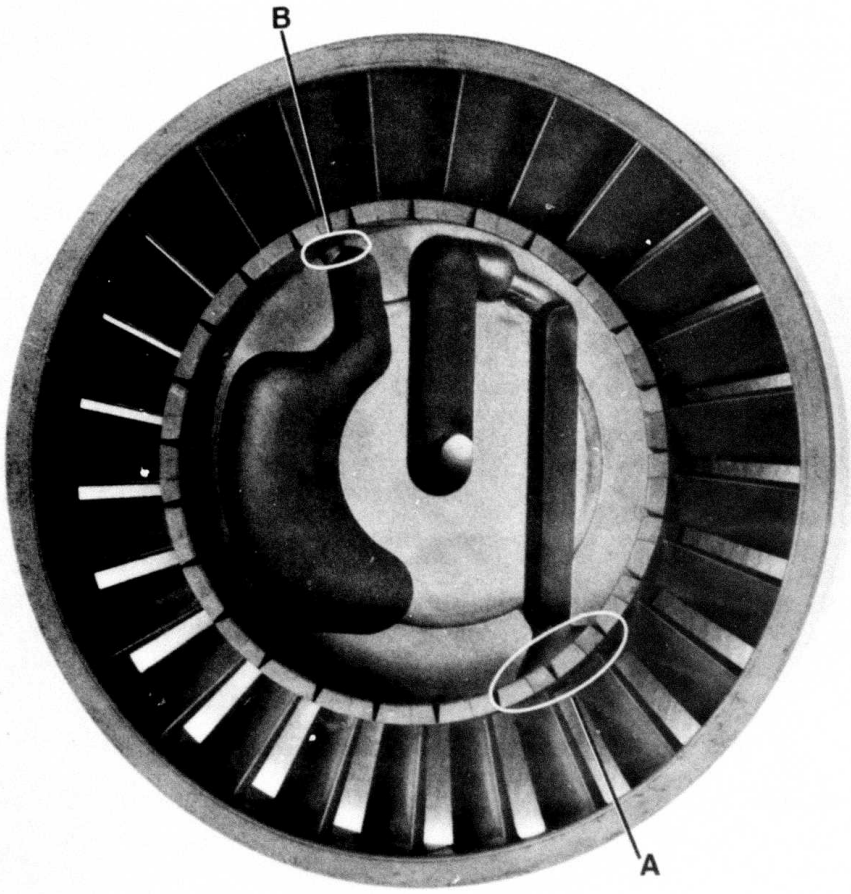

Figure 3.20 — Sprue Detail of Design D' Stator Tool

A group of visually flaw free as molded stators was produced. The green vanes and shrouds appeared to be of good quality after microscopic and visual inspection. The overflow reservoir, eliminated during this last molding run, was initially incorporated to trap gas bubbles which formed in the turbulent flow region formed as the material entered the die. It appears that the improved machine control and the pre-injection cavity vacuum reduce the need for the overflow reservoir.

Further processing of these molded stators through burnout and nitriding resulted in 26 stators of acceptable quality. Mechanical testing of these 26 components is discussed in the NDE segment of this Fabrication Section.

Silicon Carbide Stators

Several stators have been fabricated by injection molding and reaction bonding as described in the previous Report[11]. A summary of those suitable for further rig or engine testing is given in Table 3.6.

TABLE 3.6

Reaction Bonded SiC Stators

Serial Number	Density g/cc	% Free Silicon	Remarks Concerning Quality
507	3.10	12	Good
510	3.08	14	Some Molding Flaws
519	3.11	11	Excellent
520	3.15	7	One Blade Broken
528	3.16	6	Excellent

All stators were processed from a polymer filled with −600 mesh α−SiC particles except 507 which was filled with −1000 mesh α−SiC particles. Each stator was also silicided once in vacuum except 507 which required two vacuum siliciding treatments. It is estimated that all stators contain less than 2% porosity.

Nose Cones (Injection Molded)

As previously reported[11] nose cones fabricated prior to this reporting period exhibited small cracks in the center body to strut fillet and outer body to strut fillet. The cause of the cracks was traced to the movement of the outer die blocks prior to complete withdrawal of the center core pins. A rework of the die was made to eliminate this problem. The die was reworked to allow center core pin withdrawal with the die fully clamped. The outer die blocks now open only after core pin withdrawal. Hydraulic cylinders were used to clamp and move the core pins and die blocks. Cylinder configuration is shown in Figure 3.21. An initial molding run was conducted to check out tool operation. During this run it was determined that center core pins were being pushed out of the die due to material pressure. Larger hydraulic cylinders were installed to eliminate the problem. After the die was operating properly 10 nose cones were molded and visually inspected. None of the 10 showed any cracks in the strut attachment areas. These nose cones were further processed through burnout and argon sintering. To date no strut cracks are visible after processing. X-ray evaluation of the nose cones molded revealed no voids detectable in 80% of the parts. This is directly attributable to the improved clamping of the die. The tighter cavity allows higher injection pressure which tends to reduce trapped gas pockets which appear as voids. Further molding of nose cones was conducted and a large group was produced for further processing.

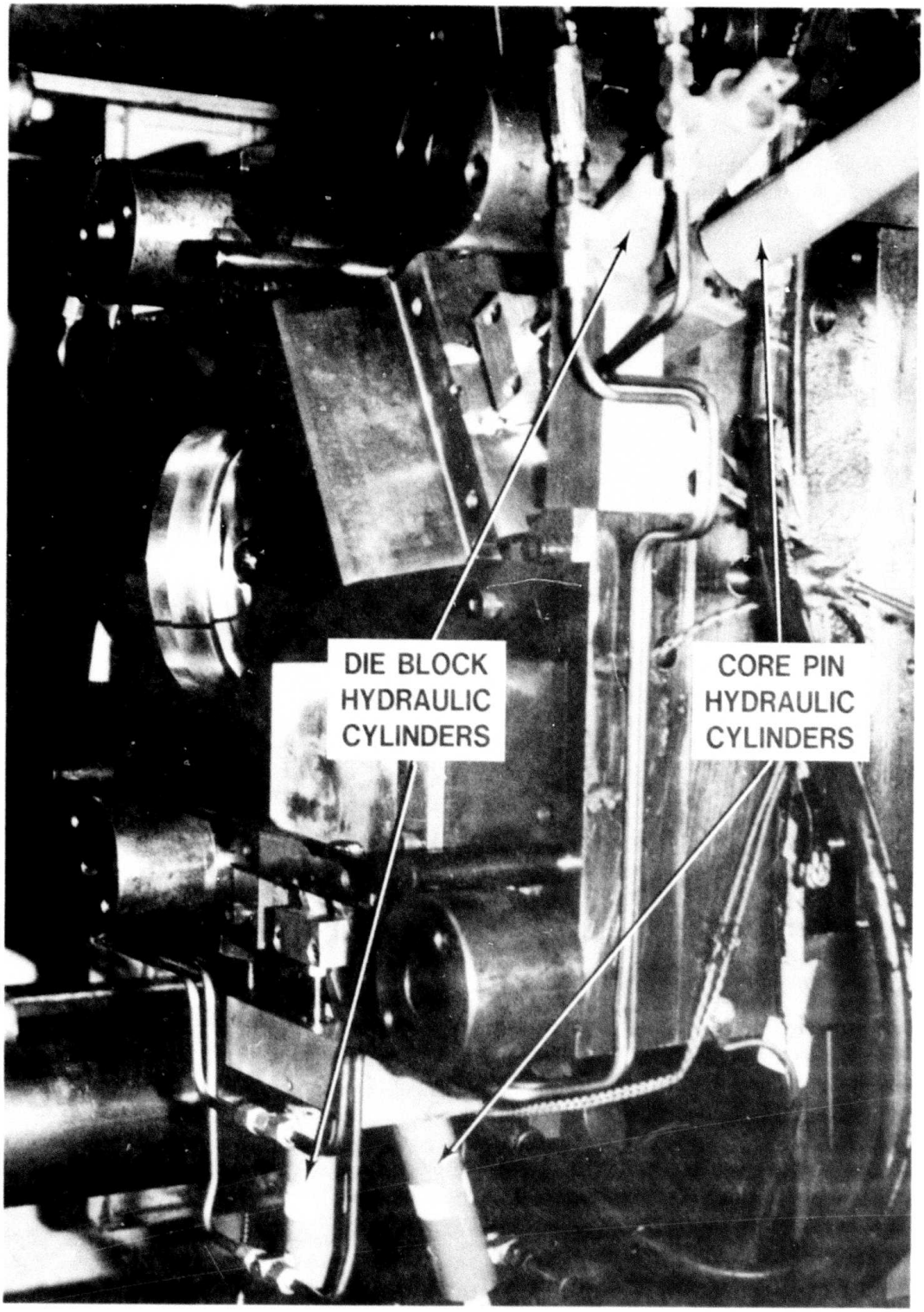

Figure 3.21 — Modified Nose Cone Tooling

Nose Cones (Slip Cast)

A slip cast nose cone feasibility investigation was conducted during this reporting period with the objective of manufacturing one nose cone for test rig evaluation. To expedite the study, an entire plaster mold system was chosen, which in turn required that the nose cone be cast in two pieces with a subsequent bonding assembly. One casting consisted of the struts and bell and the other casting consisted of the outer skirt as shown in figure 3.22. A standard blade fill silicon/silicon nitride slip was used to cast the individual units (See Blade Fill Processing section 3.1.1 this report). After casting, each piece was thoroughly dried and then argon sintered to a suitable machinability hardness. The machining required was minimal due to the dimensional accuracy of the castings; however, to facilitate the assembly process, oversized strut access holes had to be milled in the outer skirt. Once assembled the struts were bonded to the skirt using low green shrink bonding slips and using previously reported bonding procedures[13]. Another argon sinter was conducted on the bonded nose cone, after which each bond joint was optically inspected for green shrink cracks. None were observed and therefore the assembly was nitrided and final diamond ground. NDE procedures on the final product showed the part to be free of "obvious" flaws. The nose cone was then released for test rig evaluation. Details are covered in Section 3.2.2.

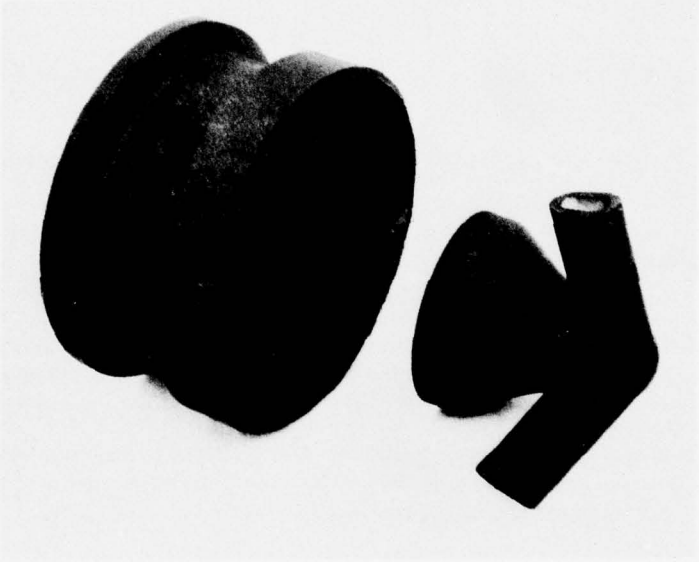

Figure 3.22 — Slip Cast Nose Cone

NDE — Stator Vane Mechanical Test Fixture

During this reporting period additional efforts were made to eliminate sticking of the loading pins in the mechanical test fixture. The loading fixture was disassembled and inspected for burrs and sharp edges which could possibly be the cause of pin to pin load variation. Pins and holes were measured in an attempt to associate pin clearance with load variation. No correlation of load variation with pin clearance variation was noted. The fixture was cleaned, reassembled, and recalibrated with essentially the same magnitude of load variation as before[11].

Twenty-six stators were screened in this fixture even though the small pin to pin variations were not eliminated. Screening conditions were 400 psi corresponding to a unit load of 20 pounds per vane. Twenty-one of twenty-six stators passed the 400 psi screening procedure. Failure usually was attributed to one or more of three types of flaws. These flaws can be characterized as 1) fillet cracks in the vane not extending to an edge, 2) leading and trailing edge cracks or, 3) surface roughness on the trailing edge of the vanes. Several of the stators had radial cracks in the vanes, and others contained shroud defects caused by poor knitting of the material during molding. This type of defect did not contribute towards mechanical failure.

3.2.2 TESTING

Introduction

The stationary hot flow path components include the combustor, turbine inlet nose cone, common first and second stage stators, and first and second stage rotor tip shrouds. In the Design D prime configuration[10], the addition of a second stage stator centering ring was made.

The ceramic flow path components, with the exception of the combustor, were extensively tested and a number of significant milestones were achieved.

The testing centered on qualification of components and subsequent steady state durability testing at 1930 and 2500°F. In addition, duty cycle transient environment testing was initiated. With the inclusion of this test, ceramic flow path components were subjected to the total thermal environments contained within the planned 200 hour durability duty cycle.

As was stated in the last report[11], the fabrication of ceramic flow path components was resumed, on a limited basis, utilizing a 2.7 g/cc density silicon nitride material for the first time for injection molding. It was primarily components from this effort which were evaluated during this reporting period.

Also evaluated was the initial silicon nitride nose cone fabricated by the slip casting process. Testing of a reaction bonded silicon carbide stator was resumed.

A summary of all flow path components evaluated during this reporting period is presented in Tables 3.7, 3.8 and 3.9.

Component Qualification

As described in previous reports[6,9,10,11], stationary ceramic flow path components are initially subjected to a qualification test before being considered acceptable for engine testing. This is done to screen out parts with gross fabrication and/or processing defects.

While the previously described 10-light test[10], appears to be sufficient for nose cones, tip shrouds, and centering rings, it appears to be inadequate for stators. Therefore in order to better qualify stators prior to engine testing, two additional tests have been incorporated as part of the stator qualification sequence. These tests were introduced in the last report[11] and have been expanded during this reporting period.

The first test subjects each stator vane in the assembly to a bending load. A schematic is shown in Figure 3.23. After some development[11] a qualification load (L_Q) of ten pounds per vane was selected. Eight 2.7g/cc density stators were subjected to this test. Subsequent 10-light testing failed vanes in two of these assemblies (1086 and 1049).

Table 3.10 summarizes the approximate size of the gross fabrication defects revealed from the 8 failed vanes (7 from 1086 and 1 from 1049). Failure of these vanes during the 10-light test after being vane bend tested, was an unacceptable result and prompted further testing utilizing a number of previously qualified and tested stators.

Stators 1049, 1086, 1099, and 1134 were vane bend tested to destruction. A total of 77 vanes were failed, of these, 13 vanes contained gross flaws in the fracture surface. The approximate flaw sizes versus failure load is shown Figure 3.24. The remaining 64 vanes were classed as flaw-free in the fracture surface. The failure load data is presented in Figure 3.25.

Two observations were made from this data concerning:

(a) prevalent location of gross flaws and

(b) vane load capability

TABLE 3.7

Summary of Nose Cone Testing

Material and Design Identification Number	Serial Number	Transient Qualification Lights	Transient Qualification Shut-downs Cold	Transient Qualification Shut-downs Hot	Transient Qualification Hours**	1930°F Durability Lights Cold	1930°F Durability Lights Hot	1930°F Durability Shut-downs Cold	1930°F Durability Shut-downs Hot	1930°F Durability Hours**	2500°F Durability Lights	2500°F Durability Hours	Miscellaneous Testing Lights	Miscellaneous Testing Hours**	Component Status	Total Time Hours**	Total Lights
Target		10	9	1	0.2	12	24	0	36	175	4	25			S	200	50
S	73												142	16.75	F	16.75	142
1	**102**	**20**	**18**	**2**	**0.5**	**49**	**36**	**21**	**64**	**245.5**					**F,B**	**246**	**105**
1	103	19	17	2	0.4	1	2		3	50.5					F,O	50.9	22
1	130					5	3	2	6	24.5					F,H	24.5	8
S	202	10	9	1	0.2	9	2	9	2	6.5	1	5.0	1	18.3	F,C,O,X	30.0	28
2	207	51	45	6	1.1	11	10		21	77.6			8	11.75	F,B	90.45	80
1	304	46	42	4	2.0								15	50.3	F,C,O,X	52.3	61
2	320												10	1.15	F,X	1.15	10
2	321	32	29	3	1.6	25		20	5	22.8			2	2.75	F,X	27.15	59
3	806	32	30	2	0.7	4			4	29.75			8	4.3	F,B	34.75	44
3	807	64	58	6	1.25										F,C,X	1.25	64
3	814	14	13	1	0.4	5			5	33.4					F,C	33.8	19
3	861*	9	9		0.25										F,C,B	0.25	9
4	871	10	9	1	0.25	4			4	57.1					F,B	57.35	14
4	872	56	50	6	1.1								29	146.05	F,C	147.15	85
4	875	10	9	1	0.25						3	4.2	2	1.85	F,B	6.3	15
4	876	10	9	1	0.25	6			6	55.1					F,B	55.35	16
5	886*	11	9	2	0.3										F	0.3	11
4	889	40	36	4	1.0										F,C	1.0	40
5	890	10	9	1	0.25	9			9	31.8					F,H	32.05	19
5	894*					8			8	8.0			3	2.2	S	10.2	11
4	903	10	9	1	0.25										F,C,X	0.25	10
5	904												7	0.5	F,X	0.5	7
5	909*												3	37.25	F,O	37.25	3
4	910	12	11	1	0.25										F,B	0.25	12
4	916	14	13	1	0.25	12			12	30.6					F,C	30.85	26
4	917	10	9	1	0.25										F,C,X	0.25	10
4	920												3	1.5	F,B,X	1.5	3
6	1006*	213	191	22	6.1										S	6.1	213
6	**1011***	**10**	**9**	**1**	**0.25**	**22**			**22**	**175.0**	**10**	**26.4**			**S**	**201.65**	**42**
6	**1018***	**12**	**11**	**1**	**0.25**	**27**			**27**	**186.7**	**2**	**7.0**			**F,H**	**193.95**	**41**
6	1023*	3	3		0.1										F	0.1	3
7	AE1*	39	9	30	1.5	5			5	36.75					F,B	38.25	44
6	1037*	10	9	1	0.25						4	8.4			F,B	8.65	14

* New entry this reporting period ** Up to at least 1930°F

Serial Numbers 73-321 are 2.2 g/cc density; 806-894 are 2.55 g/cc density; 1000 series are 2.7 g/cc density.

Key to Component Status

- F = Failed
- O = Failure occurred in other than ARPA duty cycle
- H = Part failed during handling
- S = Serviceable
- C = Cracked shroud
- B = Inner body crack
- X = Internal material flaw involved to failure

Key to Material and Design Identification Number

- S = Special experimental modification
- 1 = Short, slotted and scalloped
- 2 = Long, slotted and scalloped with thermocouple holes
- 3 = Short, design D
- 4 = Long, design D
- 5 = Angled slots 2.55 g/cc density
- 6 = Angled slots 2.7 g/cc density
- 7 = Slip cast, angled slots 2.5 g/cc density

TABLE 3.8

Summary of Stator Testing

Material Identification Number	Serial Number	Transient Qualification Lights	Transient Qualification Shut-downs Cold	Transient Qualification Shut-downs Hot	Transient Qualification Hours**	1930°F Durability Lights	1930°F Durability Shut-downs Cold	1930°F Durability Shut-downs Hot	1930°F Durability Hours**	2500°F Durability Lights	2500°F Durability Hours	Miscellaneous Testing Lights	Miscellaneous Testing Hours**	Component Status	Total Time Hours**	Total Lights
Target		10	9	1	0.2	12	24	0	36	175	4	25			S	200	50
2	421	10	9	1	0.2								3	2.80	C,X	3.00	13
2	424	10	9	1	0.25								9	2.75	C,X	3.00	19
2	428	10	9	1	0.2	17	14	6	25	103					F,C	103.2	41
2	430	10	9	1	0.2	14	13	6	21	61.5					F,C	61.7	37
5	**525***	**14**	**13**	**1**	**0.5**	**29**			**29**	**175.75**	**9**	**28.9**			**S**	**205.2**	**52**
1	715	10	9	1	0.2								6	0.1	F,V,O	0.3	16
1	751	11	10	1	0.2								2		C,V,O,X	0.2	13
2	817	34	31	3	0.75										S	0.75	34
1	820	14	13	1	0.3										C,X	0.3	14
1	841	12	11	1	0.2	6	10		16	42.8					F,C	43.0	28
1	848	11	10	1	0.2										F,H	0.2	11
1	852	23	20	3	1.7										F,O	1.7	23
1	858	12	11	1	0.2	6	10		16	42.8					F,C	43.0	28
1	865	12	11	1	0.25								2	9.5	F,V,I,O	10.15	14
1	868	12	11	1	0.25								2	9.5	F,V,I,O	10.15	14
6	879*	10	9	1	0.25						2	1.0	19	40.0	F,V,I	41.25	31
2	880	51	44	7	3.7								1	5.0	S	8.7	52
6	884	10	9	1	0.25	18			18	20.15					F,H	20.4	28
3	889	122	110	12	21.4								4	4.68	S	26.1	126
3	898*	45	9	36	1.75	5			5	36.75					S	38.5	50
1	910*										1	1.0	7	55.75	F,V,I	56.25	8
1	911	10	9	1	0.25	5			5	54.0					F,V	54.25	15
2	911A	11	10	1	0.25						1	0.25	11	21.75	F,V,I,O	22.25	23
4	912A*	10	9	1	0.25										F,C	0.25	10
4	913	16	9	7	0.5										S	0.5	16
6	921	10	9	1	0.25	9			9	8.15					F,H	8.4	19
4	924	10	9	1	0.25								21	30.5	F,V,X	30.75	31
4	927	10	9	1	0.25								7	0.5	F	0.75	17
4	936	10	9	1	0.25	5			5	10.0					S	10.25	15
4	940	10	9	1	0.25	19		6	13	32.5					F,C	32.75	29
4	943	10	9	1	0.25						3	4.2	1	1.45	F,C	5.9	14
4	945	11	9	2	0.5								1	0.03	F,O	0.53	12
4	948*	10	9	1	0.25	10			10	175.75					S	176.0	20
4	954	10	9	1	0.25	9			9	174.75					S	175.0	19
3	955	10	9	1	0.25	2			2	22.75					F,C	23.0	12
7	1037*	10	9	1	0.25										F,V	0.25	10
7	1039*	10	9	1	0.25										F,V	0.25	10
7	1049*	10	9	1	0.25										F,V	0.25	10
7	1071*	10	9	1	0.25										S	0.25	10
7	1086*	4	4		0.03										F,V,C	0.03	4
7	1096*	10	9	1	0.25	10			10	175.75					S	176.0	20
7	1099*	39	9	30	1.50	4			4	36.75					F,C	38.25	43
7	1104*	10	9	1	0.25						4	8.4			F,C,X	8.65	14
7	**1105***	**12**	**11**	**1**	**0.25**	**22**			**22**	**175.0**	**10**	**26.4**			**S**	**201.65**	**44**
7	1113*	10	9	1	0.25								3	37.25	F,O	37.5	13
7	1114*	13	12	1	0.25										F	0.25	13
7	**1117***	**10**	**9**	**1**	**0.25**	**22**			**22**	**175.0**	**10**	**26.4**			**S**	**201.65**	**42**
7	1134*	10	9	1	0.25										F,C	0.25	10
7	1135*	10	9	1	0.25										S	0.25	10

* New entry this reporting period ** Up to at least 1930°F

Serial Number 421-955 are 2.55 g/cc except for 525 which was SiC; 1000 Series are 2.7 g/cc density.

Key to Component Status

S = Serviceable C = Cracked shroud X = Internal material flaw involved in failure
F = Failed V = Vane(s) failed I = Impact failure from combustor carbon
O = Failure occurred in other than ARPA duty cycle
H = Part failed during handling

Key to Material Identification Number

1 = Nitrided in Harrup
2 = Nitrided at Vac Hyd
3 = Nitrided in Brew 100% Nitrogen
4 = Nitrided in Brew 96% Nitrogen, 4% Hydrogen
5 = Silicon Carbide
6 = Nitrided at Vac Hyd and at Ford
7 = Nitrided in Brew 96% Nitrogen, 4% Hydrogen, 2.7g/cc density

TABLE 3.9

Summary of Shroud & Centering Ring Testing

Design Identification Number	Serial Number	Transient Qualification Lights	Transient Qualification Shut-downs Cold	Transient Qualification Shut-downs Hot	Transient Qualification Hours**	1930°F Durability Lights Cold	1930°F Durability Lights Hot	1930°F Durability Shut-downs Cold	1930°F Durability Shut-downs Hot	1930°F Durability Hours**	2500°F Durability Lights	2500°F Durability Hours	Miscellaneous Testing Lights	Miscellaneous Testing Hours**	Component Status	Total Time Hours**	Total Lights
Target		10	9	1	0.2	12	24	0	36	175	4	25			S	200	40
First Shrouds																	
1	24	19	17	2	0.4	1	2		3	50.5					S	50.9	22
1	**111**	**13**	**12**	**1**	**0.2**	**61**	**41**	**34**	**68**	**245.0**					**S**	**245.2**	**115**
2	119	15	13	2	0.25										F	0.25	15
2	120	12	11	1	0.25										S	0.25	12
2	124	10	9	1	0.25										S	0.25	10
2	**134**	**10**	**9**	**1**	**0.25**	**22**			**22**	**175.0**	**10**	**26.4**			**S**	**201.65**	**42**
2	136	10	9	1	0.25	13			13	125.75					F,C	126.0	23
5	1	10	9	1	0.25								7	0.5	F	0.75	17
5	2					15			15	18.00			3	2.1	S	20.1	18
7	1	10	9	1	0.25								3	37.25	F	37.5	13
7	2	12	11	1	0.25	1			1	49.7	9	29.9			S	79.85	22
7	3	25	17	8	0.7										S	0.7	25
7	4	12	11	1	0.25										F	0.25	12
7	5	39	9	30	1.5	5			5	36.75					S	38.25	44
7	6	10	9	1	0.25										S	0.25	10
Second Shrouds																	
3	2	10	9	1	0.25										F,C	0.25	10
3	3	12	11	1	0.25						8	10.2	31	75.7	S	86.15	51
3	4	10	9	1	0.25										F,C	0.25	10
4	6												3	1.75	F	1.75	3
4	38	19	17	2	0.40	11	2		13	56.7					F	57.1	32
4	100					1	9		10	6.4			30	1.6	S	8.0	10
4	102					1	9		10	6.4					S	6.4	10
4	104												75	5.1	S	5.1	74
4	**106**	**10**	**9**	**1**	**0.2**	**61**	**41**	**34**	**68**	**245.0**					**S**	**245.2**	**112**
6	**1**	**32**	**29**	**3**	**0.7**	**22**			**22**	**175.0**	**10**	**26.4**			**S**	**202.1**	**64**
6	2	10	9	1	0.25								3	37.25	F	37.5	13
6	3	19	19		0.5										S	0.5	19
6	4	10	9	1	0.25										S	0.25	10
6	5	39	9	30	1.5	5			5	36.75					S	38.25	44
6	6										10	32.4	1	1.0	S	1.0	1
6	7	20	18	2	0.5										S	0.5	20
Centering Rings																	
8	1	10	9	1	0.2	7			7	168.	8	24.3			S	192.5	25
8	3	12	11	1	0.25	15			15	23.8					F	24.05	27
9	1	10	9	1	0.25								3	37.25	F	37.5	13
9	**2**	**12**	**11**	**1**	**0.25**	**22**			**22**	**175.0**	**10**	**26.4**			**S**	**201.65**	**44**
9	3	4	4		0.1						9	29.9	1	1.0	S	31.0	14
9	4	55	49	6	1.5										S	1.5	55
9	5	39	9	30	1.5	5			5	36.25					S	38.25	44
9	6	10	9	1	0.25										S	0.25	10

** Up to at least 1930°F Density 2.6-2.7g/cc

Key to Component Status
- S = Serviceable
- F = Failed
- C = Cracked

Key to Design Identification Number

- 1 = 1st stage design B
- 2 = 1st stage design D
- 3 = 2nd stage design D
- 4 = 2nd stage design B
- 5 = 1st stage modified engine design
- 6 = 2nd stage design D, unslotted
- 7 = 1st stage design D, unslotted
- 8 = 2nd stage stator centering ring, slotted
- 9 = 2nd stage stator centering ring, unslotted

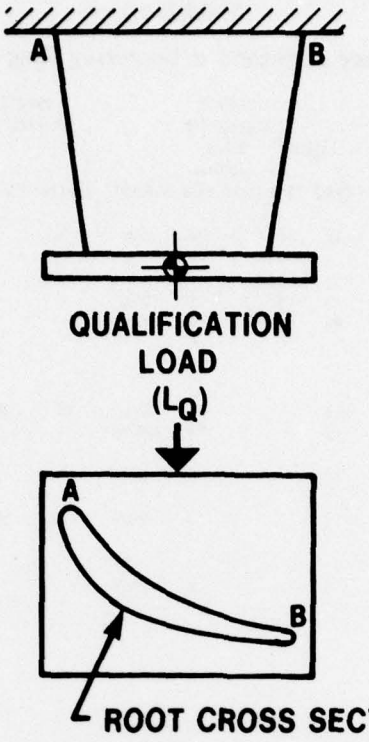

A — LEADING EDGE MAX STRESS LOCATION
B — TRAILING EDGE MAX STRESS LOCATION

Figure 3.23 — Stator Vane Loading Schematic

TABLE 3.10

Approximate Flaw Size Data

Vane Identification	Approximate Flaw Size ($In.^2$)
1049 — 22	0.025
1086 — 1	0.028
1086 — 2	0.028
1086 — 3	0.024
1086 — 7	0.016
1086 — 9	0.0075
1086 — 13	0.0075
1086 — 25	0.028

In reviewing the location of gross fabrication defects in loaded-to-failure vanes (Figure 3.24) it was noted that a majority were not located at the leading or trailing edges, but rather in the heavy, central interior section. There was a tendency for this type flaw to surface on the pressure side of the vane. From a qualification load standpoint, the resulting stress in this area is minimal due to the close proximity of the flaw to the junction of the principal axes. Therefore the vane bend test (10 pounds applied load) did not eliminate all the grossly flawed vanes that were destined to fail during the subsequent 10-light test.

In reviewing the vane load capability (Figures 3.24 and 3.25) it was noted that a majority of the vanes (66 out of 77) successfully withstood an applied load of greater than 19 pounds. Of the 11 which did not, 7 contained the previously noted central interior flaw.

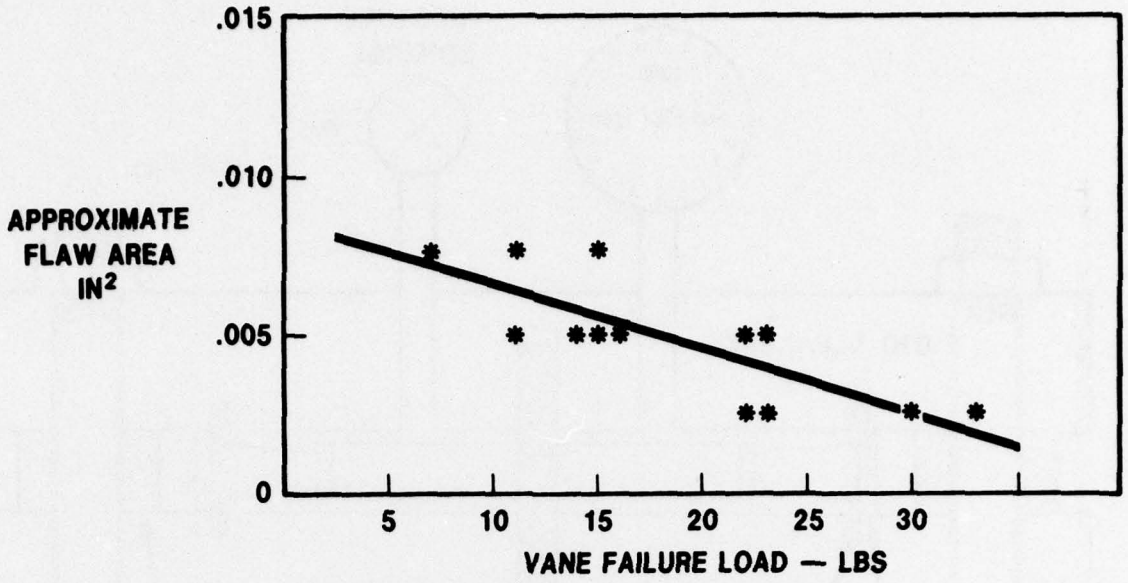

Figure 3.24 — Flaw Size Versus Failure Load

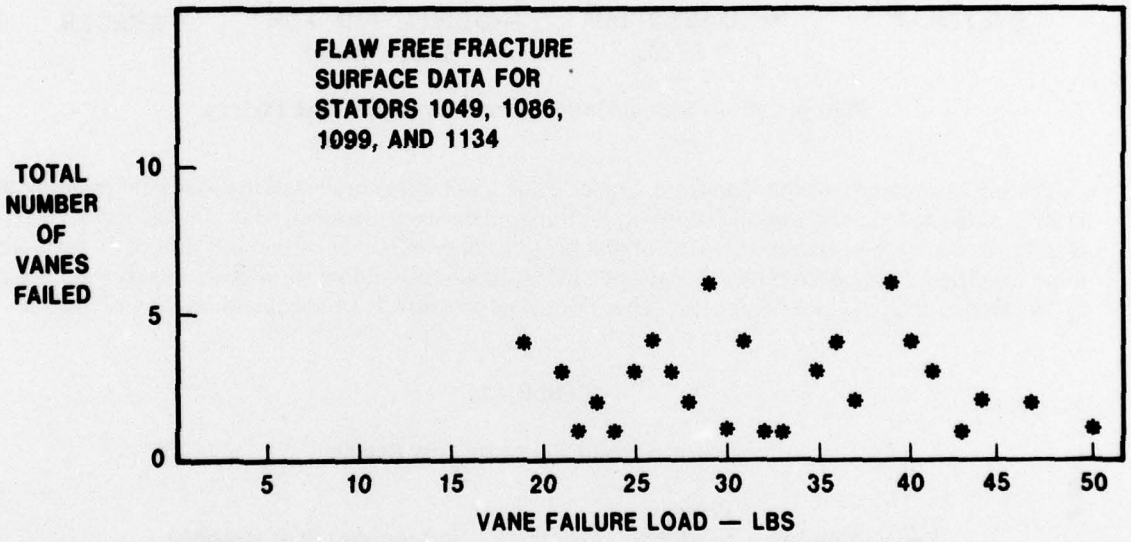

Figure 3.25 — Flaw Free Vane Failure Loads

These observations indicated that an increase in the qualification load to 19 pounds could enhance the screening out of poor quality vanes without jeopardizing quality components. To verify this, 5 stator assemblies were subjected to a 19 pound/vane qualification load and subsequently 10-light tested. Vanes in two of these stator assemblies failed during the 10-light test. This result was therefore still not satisfactory and an effort continues in this area.

The second of these tests subjects the stator outer shroud to an internal pressure using the fixture shown in Figure 3.26. A tensile stress is produced in the shroud to screen the outer shroud for unacceptable defects. During this reporting period, an effort was made to establish the internal pressure which accomplishes the screening purpose.

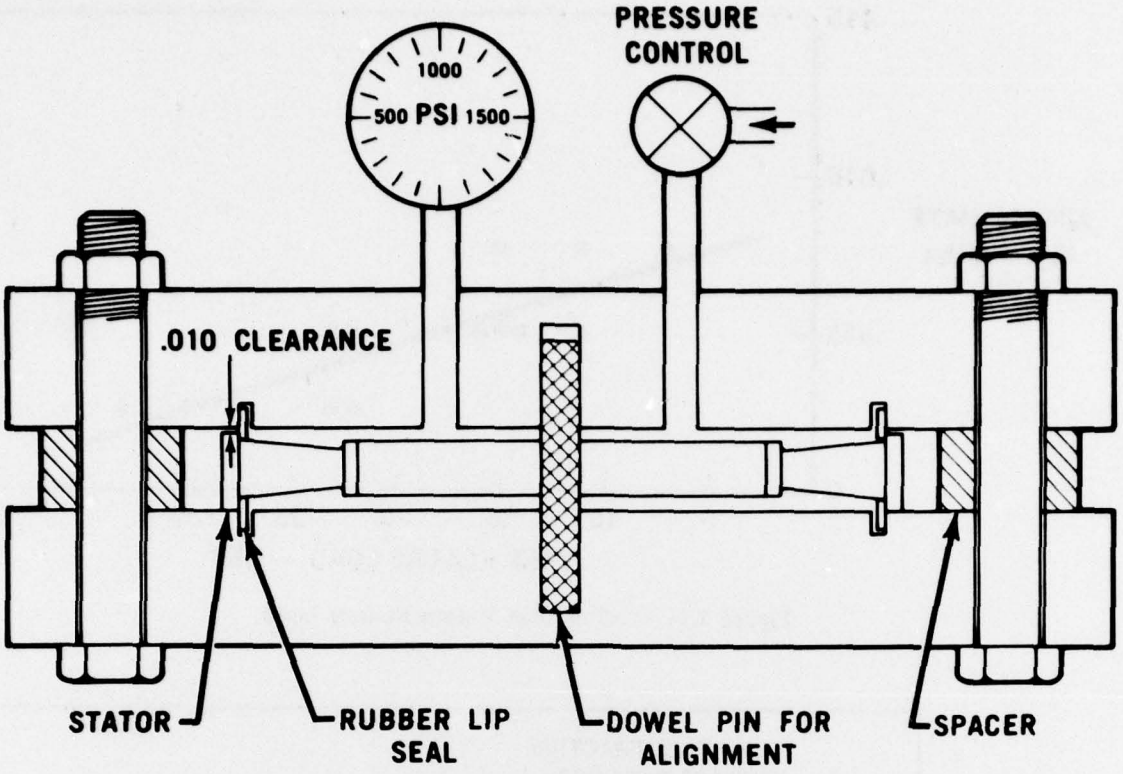

Figure 3.26 — Stator Outer Shroud Pressure Test Fixture

Table 3.11 summarizes the data from 2.7g/cc stator assemblies subjected to the shroud pressure test. Details of the test rig and establishment of the initial pressure were covered in the last report[11]. The results show that the original pressure of 100 psi did not adequately screen out defective parts since three qualified components (1086, 1104, and 1134) subsequently failed through gross fabrication flaws in the shroud during the 10-light test. Therefore, the pressure load specification was reviewed.

TABLE 3.11

Stator Shroud Pressure Test Results

Stator Number	Pressure Load PSI	Result	Subsequent Test Result(s)
1049	100	OK	No Shroud fail thru 10-light test.
1086	↑	↑	(1) shroud crack during 10-lights.
1099	↑	↑	No Shroud fail thru 10-light test.
1105	↑	↑	No Shroud fail thru 10-light test.
1113	↑	↑	No Shroud fail thru 10-light test.
1114	↑	↑	No Shroud fail thru 10-light test.
1117	↑	↑	No Shroud fail thru 10-light test.
1134	↑	↑	(1) shroud crack during 10-lights.
1037	↑	↑	No Shroud fail thru 10-light test.
1039	↓	↓	No Shroud fail thru 10-light test.
1104	100	OK	(1) shroud crack during 10-lights.
1041	200	Fail	
1071	200	OK	No Shroud fail thru 10-light test.
1135	200	OK	No Shroud fail thru 10-light test.

A bracketing of shroud screening stress was previously established between 2000 psi (100 psi internal pressure) and 9000 psi (450 psi internal pressure[11]). The original pressure load specification was chosen as the minimum of this bracketing. In reviewing the specification, it was deemed advisable to increase the load to 200 psi applied internal pressure. Only three stator assemblies have been tested at this load (See Table 3.11) and thus it has not yet been established that the 200 psi load will adequately screen out defective stator shrouds. Parts will continue to be qualified at this load until its validity has been established.

As a final step in the qualification sequence, stators are subjected to the previously noted 10-light test[10]. A summary of 2.7g/cc stator qualification sequence test results is provided in Table 3.12.

TABLE 3.12

Summary of Stator Qualification Sequence Test Results

	Vane Bend Test		Shroud Press. Test Psi		10-Light Test	
Comp. Ident.	Vane Load	Results	Press. Load	Results	Light Sched.	Results
1037	19	OK	100	OK	10	2VF
1039	19	OK	100	OK	10	1VF
1041	19	1VF	200	SF	—	—
1049	10	OK	100	OK	10	1VF
1055	10	5VF	100	OK	—	—
1056	—	—	—	—	—	—
1071	19	2VF	200	OK	10	OK
1086	10	OK	100	OK	10	7VF/SF
1096	—	—	—	—	10	OK
1099	10	OK	100	OK	10	OK
1104	19	OK	100	OK	10	SF
1105	10	OK	100	OK	10	OK
1111	19	6VF	—	—	—	—
1113	10	OK	100	OK	10	OK
1114	10	OK	100	OK	10	OK
1117	10	OK	100	OK	10	OK
1134	10	1VF	100	OK	10	SF
1135	19	2VF	200	OK	10	OK

VF = Vane Failure
SF = Shroud Failure

Steady State Durability

After completion of qualification testing, components may be subjected to static steady state durability testing in engines and/or test rigs at two turbine inlet temperature levels — 1930 and 2500°F. (The program goal is 200 hours durability — 175 hours at 1930°F and 25 hours at 2500°F.) During the past nine months, a number of significant durability test results have been achieved.

1930°F Durability

A set of ceramic stationary flow path components completed 175 hours at 1930°F average turbine inlet temperature. Data on the specific components are contained in Table 3.13. The nose cone and stator assemblies after test are shown in Figure 3.27.

TABLE 3.13

175 Hour Flowpath Components

Design D' Flowpath Components	Serial No.	Density g/cc	Total Hrs.	Total Lites	Total % Wt. Gain
Nose Cone	1018	2.7	176	20	0.406
First Stator	948	2.55	176	20	0.185
First Shroud	136/2	2.7	126/50	20	2.89/0.68
Second Stator	1096	2.7	176	20	0.65
Centering Ring	3/1	2.7	8/168	20	0.001/0.055

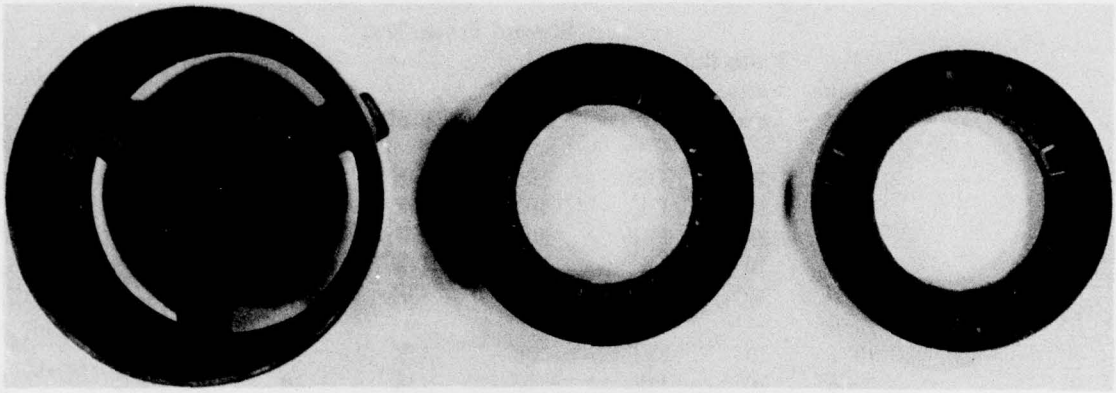

Figure 3.27 — Flowpath Components after 175 Hours at 1930°F

The last report[11] presented an accumulation of weight gain versus time data for 2.55g/cc density injection molded silicon nitride stators. The 175 hour test provided additional 2.55g/cc weight gain data and initial 2.7g/cc weight gain data. In the case of the 2.7g/cc material, data was acquired for the nose cone as well as the stator. In addition, weight gain data for the slip cast silicon nitride first stage shroud was obtained. These data are presented in Figure 3.28. As a reference, the "maximum observed", "minimum observed", and "failure zone" notations established by the prior 2.55g/cc data have been retained. Note that all three injection molded components from the 175 hour test exhibited weight gains below the previous minimum observed line.

The weight gain data for the slip cast first stage shroud (136) is also shown in Figure 3.28. The cross-hatched failure zone was established from injection molded silicon nitride 2.55g/cc density stator data and may have no relationship to slip cast silicon nitride components. However, the rate of weight gain versus time of the slip cast first shroud was of concern during the test. This component did fail between 110 and 126 hours and gained 2.89% weight. Another first stage shroud was installed in order to complete the test.

The rate of weight gain as a component selection criteria and the total percent weight gain as a component replacement criteria remain as interesting possibilities. Further data will be acquired in this area as testing continues.

Steady state testing, at 1930°F, of the reaction bonded silicon carbide stator was conducted during the past nine months. Silicon carbide stator 525 successfully completed 175 hours. The weight gain was negligible. Testing of this component at 2500°F is covered in the next section.

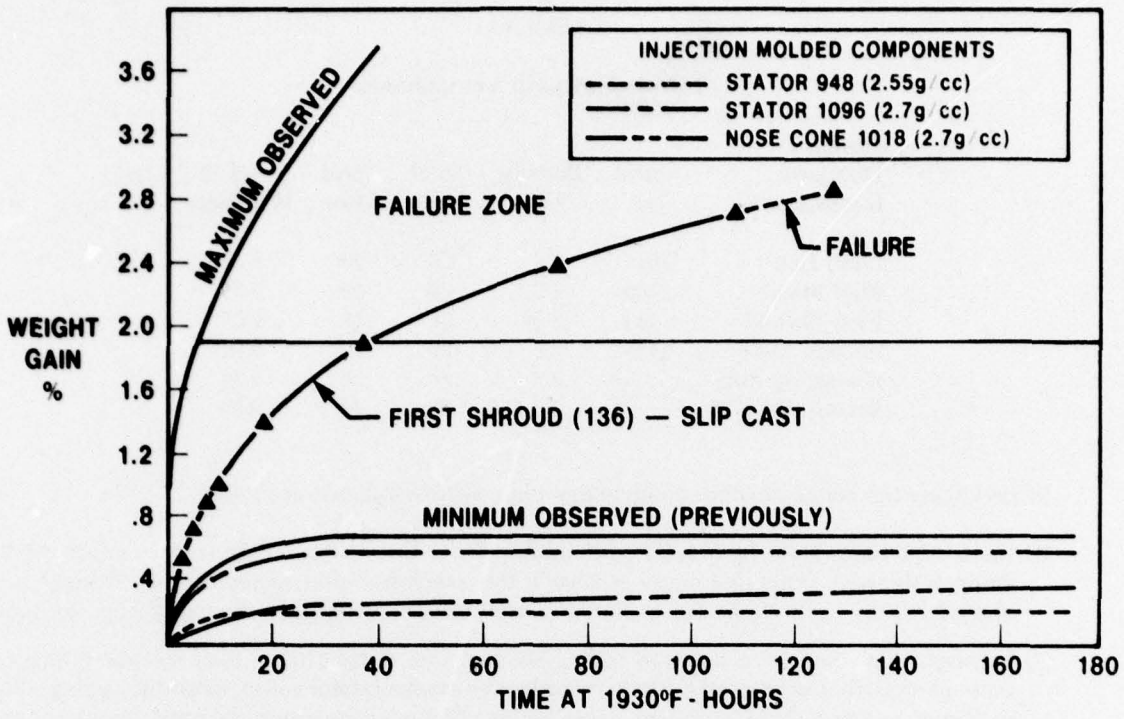

Figure 3.28 — Percent Weight Gain versus Time Data for 175 Hour, 1930°F Components

2500°F Durability

Another set of ceramic stationary flow path components completed 25 hours at 2500°F average turbine inlet temperature (See Figure 3.29). Data on the specific components are contained in Table 3.14.

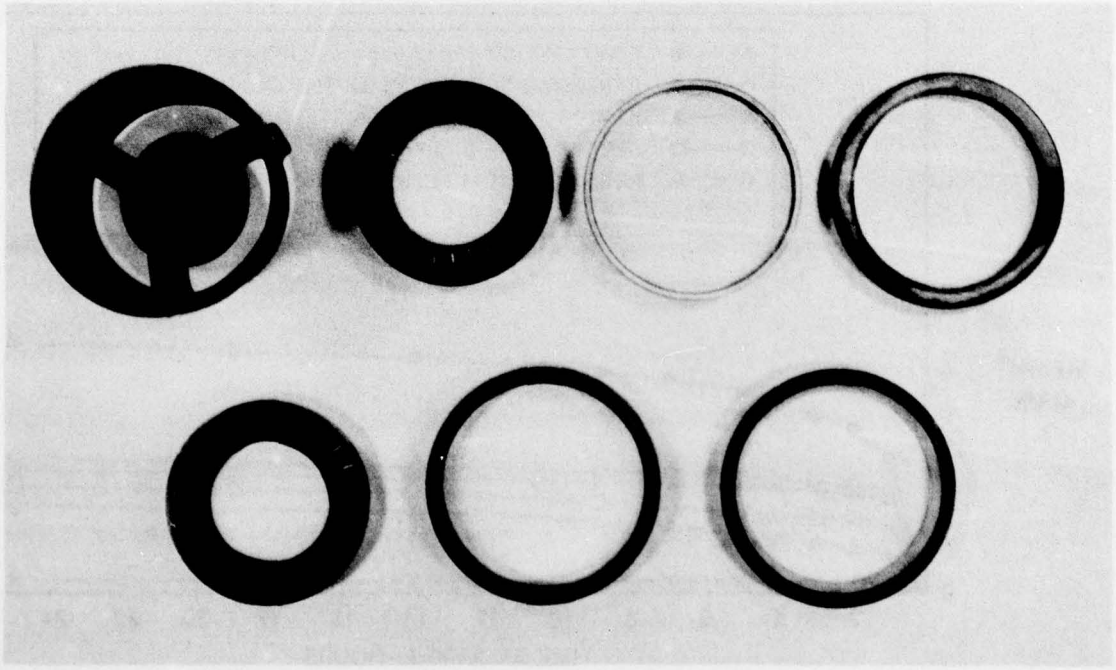

Figure 3.29 — Flowpath Components after 25 Hours at 2500°F

TABLE 3.14

25 Hour Flowpath Components

Design D' Flowpath Components	Serial No.	Density g/cc	Total Hrs.	Total Lites	Total % Wt. Gain
Nose Cone	1011	2.7	26	20	0.22
First Stator	1105	2.7	26	20	0.30
First Shroud	134	2.55	26	20	0.64
Second Stator	1117	2.7	26	20	0.02
Centering Ring	2	2.7	26	20	0.34
Second Shroud	1	2.7	26	39	0.26

In reviewing the status of these components after test, two points are noted:

(1) the second stage rotor tip shroud contained, prior to test, a radial O.D. surface crack not fully through the part; after five hours at 2500°F this crack had propagated radially through to the shroud I.D. the part continued to function and no further change was noted after 25 hours.

(2) an inspection after three hours of testing showed first stator 1105 to have a crack through the outer shroud; for purposes of radially retaining the cracked stator a thin, loose-fitting ring (shown in Figure 3.29 as a first stator insulator) was installed over the stator; the remaining 22 hours at 2500°F were completed with no change in the stator integrity.

As was the case with the 175 hour, 1930°F durability components, weight gain versus time at temperature data was accumulated. Figure 3.30 documents this data for the flow path components tested for 25 hours at 2500°F. This is the initial data obtained on engine components at this temperature for extended times. The only observation to be made at this point is that weight gain rates and total percent weight gains after 25 hours are comparable to the data obtained on successful 1930°F durability tested components.

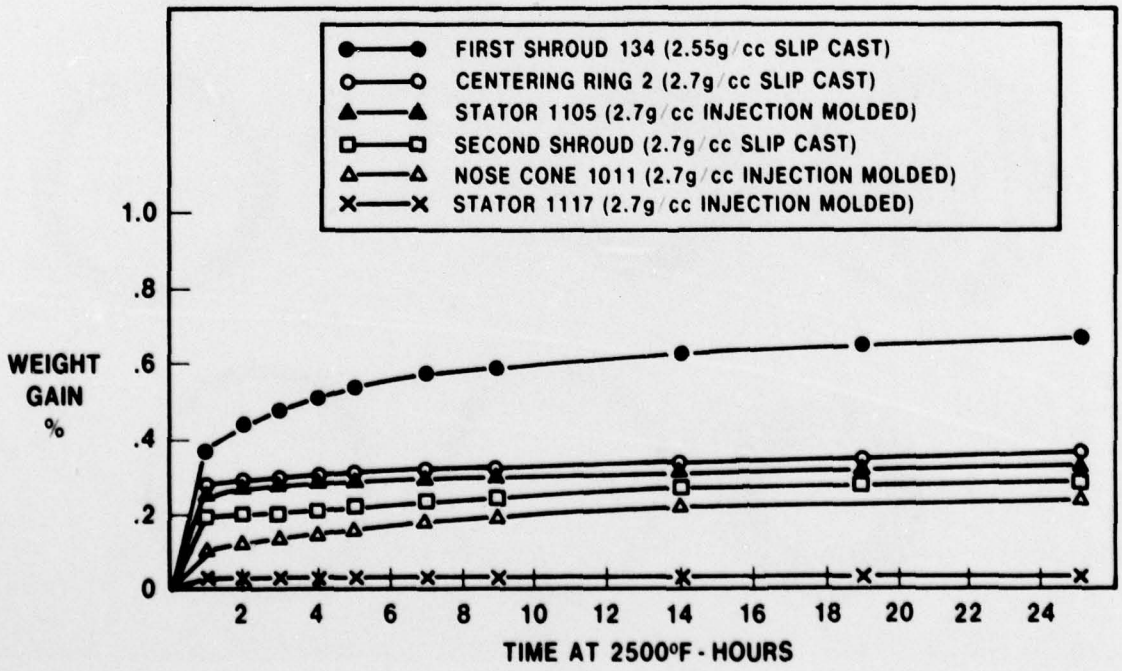

Figure 3.30 — Percent Weight Gain versus Time Data for 25 Hour, 2500°F Components

With regard to disposition of the ceramic stationary flow path components which completed the 25 hour test, the following course of action was implemented. All components were tested at 1930°F with a goal of achieving 175 hours. This satisfies the steady state durability goal of 200 hours for one set of ceramic flow path components. A summary of the data for these components is shown in Table 3.15.

TABLE 3.15

1930°F Durability Testing of 25 Hour, 2500°F Flowpath Components

	Serial No.	Density g/CC	Hrs. @ 2500° F	Hrs. @ 1930° F	Total S. S. Durability Hours	Total Lites	Total % Weight Gain
Nose Cone	1011	2.7	26	175	202	42	0.25
First Stator	1105	2.7	26	175	202	44	0.75
First Shroud	134	2.55	26	175	202	42	0.87
Second Stator	1117	2.7	26	175	202	42	0.23
Centering Ring	2	2.7	26	175	202	44	0.99
Second Shroud	1	2.7	26	175	202	64	0.29

Silicon carbide stator 525, which successfully completed 175 hours at 1930°F, was tested at 2500°F. A total of 25 hours was completed. Thus stators of two different materials, injection molded silicon nitride and reaction bonded silicon carbide, have now completed the steady state durability goal of 200 hours.

Duty Cycle Transients

In addition to the steady state environments of 1930 and 2500°F, the outlined duty cycle contains a specific number of transients. During the 200 hours, a goal of 39 start-up and shutdowns was established. The 39 start-ups are made of 13 cold starts and 26 hot starts. The 39 shutdowns are all from a hot steady state condition.

During the past six months, a set of qualified ceramic stationary flow path components was successfully subjected to the total transient requirements contained in the 200 hour duty cycle. This is referred to as extended light off testing. Data on the specific components are contained in Table 3.16.

TABLE 3.16

Extended Light-Off Flowpath Components

Design D' Flowpath Components	Serial No.	Density g/cc	Duty Cycle Transients Cold Lites	Hot Lites	Total Lites	Total % Wt. Gain
Nose Cone	AE1	2.7	13	26	39	0.23
First Stator	898	2.55	13	26	39	0.55
First Shroud	5	2.7	13	26	39	0.18
Second Stator	1099	2.7	13	26	39	0.17
Centering Ring	5	2.7	13	26	39	0.19
Second Shroud	5	2.7	13	26	39	0.24

4.0 REFERENCES

1. McLean, A. F., Fisher, E. A., Harrison, D. E., "Brittle Materials Design, High Temperature Gas Turbine". AMMRC-CTR-72-3, Interim Report, March, 1972.

2. McLean, A. F., Fisher, E. A., Bratton, R. J., "Brittle Materials Design, High Temperature Gas Turbine". AMMRC-CTR-72-19, Interim Report, September, 1972.

3. McLean, A. F., Fisher, E. A., Bratton, R. J., "Brittle Materials Design, High Temperature Gas Turbine". AMMRC-CTR-73-9, Interim Report, March, 1973.

4. McLean, A. F., Fisher, E. A., Bratton, R. J., "Brittle Materials Design, High Temperature Gas Turbine". AMMRC-CTR-73-32, Interim Report, September, 1973.

5. McLean, A. F., Fisher, E. A., Bratton, R. J., "Brittle Materials Design, High Temperature Gas Turbine". AMMRC-CTR-74-26, Interim Report, April, 1974.

6. McLean, A. F., Fisher, E. A., Bratton, R. J., "Brittle Materials Design, High Temperature Gas Turbine". AMMRC-CTR-74-59, Interim Report, September, 1974.

7. McLean, A. F., Fisher, E. A., Bratton, R. J., Miller, D. G., "Brittle Materials Design, High Temperature Gas Turbine". AMMRC-CTR-75-8, Interim Report, April, 1975.

8. McLean, A. F., Fisher, E. A., Bratton, R. J., Miller, D. G., "Brittle Materials Design, High Temperature Gas Turbine". AMMRC-CTR-75-28, Interim Report, September, 1975.

9. McLean, A. F., Baker, R. R., Bratton, R. J., Miller, D. G., "Brittle Materials Design, High Temperature Gas Turbine". AMMRC-CTR-76-12, Interim Report, April, 1976.

10. McLean, A. F., Baker, R. F., "Brittle Materials Design, High Temperature Gas Turbine". AMMRC-CTR-76-31, Interim Report, October, 1976.

11. McLean, A. F., Fisher, E. A., "Brittle Materials Design, High Temperature Gas Turbine". AMMRC-CTR-77-20, Interim Report, June, 1977.

12. Miller, D. G., "Brittle Materials Design, High Temperature Gas Turbine". AMMRC-CTR-76-32, Final Report, December, 1976.

13. Goodyear, M. U. and Ezis, A., "Joining of Turbine Engine Ceramics" in *Advances in Joining Technology*, Burke, J. J.; Gorum, A. E.; and Tarpinian, A. ids., Chestnut Hill, Mass.: Brook Hill Publishing Company, (1976), 113-154.

UNCLASSIFIED

SECURITY CLASSIFICATION OF THIS PAGE (When Data Entered)

REPORT DOCUMENTATION PAGE		READ INSTRUCTIONS BEFORE COMPLETING FORM
1. REPORT NUMBER AMMRC TR 78-14	2. GOVT ACCESSION NO.	3. RECIPIENT'S CATALOG NUMBER
4. TITLE (and Subtitle) Brittle Materials Design, High Temperature Gas Turbine Volume 1 Ceramic Component Fabrication & Demonstration		5. TYPE OF REPORT & PERIOD COVERED Interim Report Number 12 1-1-77 to 9-30-77
		6. PERFORMING ORG. REPORT NUMBER
7. AUTHOR(s) A. F. McLean, Ford Motor Company R. R. Baker, Ford Motor Company		8. CONTRACT OR GRANT NUMBER(s) DAAG 46-71-C-0162
9. PERFORMING ORGANIZATION NAME AND ADDRESS Ford Motor Company, Dearborn, MI 48121		10. PROGRAM ELEMENT, PROJECT, TASK AREA & WORK UNIT NUMBERS D/A Project: ARPA Order 1849 AMCMS Code: Agency Accession: DA OD 4733
11. CONTROLLING OFFICE NAME AND ADDRESS Army Materials and Mechanics Research Center Watertown, Massachusetts 02172		12. REPORT DATE March, 1978
		13. NUMBER OF PAGES 65
14. MONITORING AGENCY NAME & ADDRESS(if different from Controlling Office)		15. SECURITY CLASS. (of this report) Unclassified
		15a. DECLASSIFICATION/DOWNGRADING SCHEDULE

16. DISTRIBUTION STATEMENT (of this Report)

Approved for public release, distribution unlimited.

17. DISTRIBUTION STATEMENT (of the abstract entered in Block 20, if different from Report)

18. SUPPLEMENTARY NOTES

19. KEY WORDS (Continue on reverse side if necessary and identify by block number)

Gas Turbine Engine	Silicon Nitride
Brittle Design	Silicon Carbide
Ceramics	Non-Destructive Test
High Temperature Materials	Mechanical Properties

20. ABSTRACT (Continue on reverse side if necessary and identify by block number)

(See reverse side)

DD FORM 1 JAN 73 1473 EDITION OF 1 NOV 65 IS OBSOLETE

UNCLASSIFIED

SECURITY CLASSIFICATION OF THIS PAGE (When Data Entered)

ABSTRACT

In fiscal year 1977, ERDA joined forces with DARPA to support this project. The progress made on the DARPA Ceramic Turbine Testing Program is presented in this volume while the progress on the ERDA Ceramic Turbine Technology and Ceramic Turbine Materials and NDE Technology Programs is presented in Volume 2.

Duo-density rotor fabrication continued with over 600 rotor blade rings injection molded utilizing the automatic solid state control system. Yield of blade rings having no visible defects in the green, as molded, state was over 70%. Controlling the boron nitride thickness during blade fill processing coupled with a modification of the hot press graphite tooling greatly improved the hot press bonding process. The yield of flaw-free hot press bondings with these changes was 70%. This represents the most significant improvement in the yield hot press bondings to date. Finish machining of rotors continued as did non-destructive evaluation. Blade bend testing was used to monitor the quality of blade ring nitriding to insure that only the higher quality nitrided blade rings were used to fabricate rotors for testing.

Eleven duo-density ceramic turbine rotors were cold spin tested to qualify them for further hot running. Ten of the eleven reached over 50,000 rpm without failing blades, with one rotor successfully qualified to over 70,000 rpm after failing one blade at 65,640 rpm.

Development of the hot spin rigs continued. A combustor flame-out problem and a durability problem with the rotor tip shroud/failure detector were resolved. In further development of the hot spin rig, a number of ceramic and metal rotors were tested accumulating 26 hours and 68 hours respectively.

An important engine test of a duo-density silicon nitride rotor was accomplished. Rotor 1195, with the associated stationary ceramic components (nose cone, stator and tip shrouds), was successfully operated at an average Turbine Inlet Temperature (T.I.T.) of 2200°F and 45,000 rpm for 10 hours without incident. This same rotor, with 27 full length aerodynamically functional blades and stationary flowpath, was subsequently run for 25 hours at 2250°F average T.I.T. plus 1-1/2 hours at over 2500°F average T.I.T. all at 50,000 rpm. Despite a cautious shutdown a catastrophic failure occurred during the shutdown of the engine due to an overtemperatured metal component used to mount the ceramic rotor. The total hot time on the rotor was over 37 hours, all but a few minutes at a T.I.T. of 2200°F or higher, at speeds of 45,000 to 50,000 rpm, including 1-1/2 hours at 50,000 rpm and over 2500°F T.I.T. This unprecedented test is the first time a ceramic rotor has been operated at these speed/temperature/time conditions.

Fabrication development on injection molding of stators and nose cones of 2.7g/cc density was continued on a limited basis. Some additional reaction sintered silicon carbide stators were also fabricated because of promising test results previously presented. Limited development of injection molded and slip cast nose cones was continued.

Testing of stationary components continued in both qualification and durability rigs. Stators were subjected to more severe qualification tests as the vane bend load was increased from 10 to 19 pounds and the outer shroud pressure load was increased from 100 to 200 psi. Weight gains of components were monitored during hot testing at 1930 and 2500°F and found to be below previously observed values for several injection molded parts. Over 1000 hours of hot testing was accumulated on stators during this reporting period.

A complete set of silicon nitride stationary components consisting of a nose cone, two stators, two rotor tip shrouds and a second-stage stator centering ring completed the program objective of 175 hours at 1930°F plus 25 hours at 2500°F with over 40 lights. In addition, a silicon carbide stator successfully completed over 175 hours at 1930°F plus over 28 hours at 2500°F with 52 lights. Stators of two different materials, injection molded silicon nitride and reaction bonded silicon carbide, have now completed the program durability goal of 200 hours.